

2014

Mechanical and Transport Properties of Alkali-Activated Natural Pozzolans as Sustainable Binders

Brittany Radke
radkeb4@unlv.nevada.edu

Follow this and additional works at: <https://digitalscholarship.unlv.edu/award>

 Part of the [Civil Engineering Commons](#), [Construction Engineering and Management Commons](#), [Structural Engineering Commons](#), and the [Structural Materials Commons](#)

Repository Citation

Radke, B. (2014). Mechanical and Transport Properties of Alkali-Activated Natural Pozzolans as Sustainable Binders.

Available at: <https://digitalscholarship.unlv.edu/award/19>

This Thesis is protected by copyright and/or related rights. It has been brought to you by Digital Scholarship@UNLV with permission from the rights-holder(s). You are free to use this Thesis in any way that is permitted by the copyright and related rights legislation that applies to your use. For other uses you need to obtain permission from the rights-holder(s) directly, unless additional rights are indicated by a Creative Commons license in the record and/or on the work itself.

This Thesis has been accepted for inclusion in Calvert Undergraduate Research Awards by an authorized administrator of Digital Scholarship@UNLV. For more information, please contact digitalscholarship@unlv.edu.

MECHANICAL AND TRANSPORT PROPERTIES OF ALKALI-ACTIVATED NATURAL
POZZOLANS AS SUSTAINABLE BINDERS

By

Brittany Radke

Honors Thesis submitted in partial fulfillment

for the designation of Department Honors

Civil and Environmental Engineering and Construction Management

Dr. Nader Ghafoori

Dr. Mohamed Kaseko

Dr. Andrew Hanson

Howard R. Hughes College of Engineering

University of Nevada, Las Vegas

May, 2014

Abstract

OPC production accounts for 5 to 7% of the global carbon dioxide (CO₂) emissions, contributing to global warming. The desire to reduce CO₂ emissions and produce more durable concrete has given impetus to search for new binders. It is suggested that alkali-activated natural pozzolans have the potential for use as a sustainable replacement for OPC in concrete.

The current study presented herein evaluated fresh, mechanical, and transport properties of alkali-activated natural pozzolan mortars containing various concentrations of sodium hydroxide solutions as an alkaline activator. To this aim, alkali-activated natural pozzolan mortars were made with concentrations of sodium hydroxide (NaOH) of 2.5, 5, 7.5, 10 and 12.5 molar (M) and by using various solution-to-binder ratios (s/b ratios) of 0.50, 0.54, and 0.58 with a fine aggregate-to-binder ratio of 2.

The produced mortar samples were sealed-cured for 3 hours at 60°C, and then de-molded and cured at 80°C until testing at different ages of 1, 3, and 7 days. Another group of samples were cured in a curing room for 28 days. Various tests were conducted on the alkali-activated natural pozzolan mortar samples including flow spread, compressive strength, flexural strength, absorption, void content, and rapid chloride migration.

The 12.5 M 0.58 s/b ratio mixture achieved the highest overall compressive strength after seven days of sealed curing. The sealed curing environment was found to be most conducive to strength gain, as the exposed condition led to dehydration within the samples and the moisture condition did not allow for full removal of excess water, reducing bond formation. As the NaOH concentration increased, the compressive and flexural strengths increased, while the flow, void content, and chloride migration decreased. Increasing the s/b ratio reduced compressive and flexural strengths and increased flow, void content, and chloride migration.

Acknowledgments

I would like to thank Dr. Ghafoori for offering me the opportunity to perform this research and for all of his support and guidance throughout the study. I also have to thank the members of Dr. Ghafoori's research team and the facility managers within the Howard R. Hughes College of Engineering for all of their assistance through the experimentation and writing of this thesis. I could not have done it without their instrumental help. I would also like to acknowledge Dr. Hanson and Dr. Kaseko for taking time to review my thesis and act as members of my thesis committee. I have learned a great deal from all of my committee members and I am thankful for the opportunity I had to work with each of them. The Nevada Cement Company generously donated the natural pozzolans for this study, so I would like to thank them for all of their support. This research was partially funded by NSF Grant # EPS-0814372 "Nevada Infrastructure for Climate Change Science, Education, and Outreach," so I would like to thank the National Science Foundation for their support as well.

I also need to acknowledge my friends and family that have supported me throughout this journey. Without their encouragement, I would not have been able to complete this project.

This thesis is dedicated to my late grandmother, Rose Ihlenfeld. From a young age, she taught me that, “it’s a small world after all,” and that nothing is impossible.

I would not be the person I am today without her.

Table of Contents

List of Tables	vi
List of Figures	vii
Introduction	1
1. Literature Review	1
1.1 Sustainability	1
1.2 Durability	2
1.3 History of Pozzolanic Materials	3
1.4 Chemistry of Pozzolanic Materials	4
1.5 Effect of Temperature	6
1.6 Mechanical Strength	7
1.7 Transport Properties	9
2. Research Objectives	10
3. Materials and Experimental Program	10
3.1 Materials	11
3.2 Mortar Preparation	13
3.3 Flow	14
3.4 Compressive and Flexural Strengths	14
3.5 Density/Absorption/Voids	16
3.6 Rapid Chloride Penetration Test	18
3.7 Rapid Migration Test	19
4. Results and Discussion	21
4.1 Fresh Properties – Flow and Density	21
4.2 Compressive Strength	23
4.2.1 Effect of Curing	25
4.2.2 Effect of NaOH Concentration	34
4.2.3 Effect of Solution-to-Binder Ratio	42
4.2.4 Curing Room Samples	52
4.3 Flexural Strength	54
4.4 Density/Absorption/Voids	57
4.5 Rapid Chloride Penetration Test	60
4.6 Rapid Migration Test	64
5. Conclusion and Recommendations	67
5.1 Fresh Properties – Flow and Density	68
5.2 Compressive Strength	68
5.3 Flexural Strength	69
5.4 Density/Absorption/Voids	69
5.5 Rapid Chloride Penetration Test	69
5.6 Rapid Migration Test	70
5.7 Recommendations	70

6. Appendices.....	72
Appendix A: References	72
Appendix B: Flow Data.....	75
Appendix C: Compressive Strength Data	76
Appendix D: Density/Absorption/Void Data	81
Appendix E: RCPT Data.....	84
Appendix F: RMT Data	85

List of Tables

Table 1: Chemical Composition (oxide percent) of the Materials Used in this Study	12
Table 2: Amount Finer Than Each Laboratory Sieve, Mass Percent.....	13
Table 3: Average Compressive Strengths.....	24
Table 4: Curing Room Average Compressive Strengths	53
Table 5: Flexure Properties	54
Table 6: Average Density, Absorption, and Void Results.....	57
Table 7: Average RCPT Results	61
Table 8: Average RMT Results	64
Table 9: Flow Results	75
Table 10: 2.5 M Compressive Strength Data.....	76
Table 11: 5.0 M Compressive Strength Data.....	77
Table 12: 7.5 M Compressive Strength Data.....	78
Table 13: 10.0 M Compressive Strength Data	79
Table 14: 12.5 M Compressive Strength Data	80
Table 15: 0.50 S/B Ratio Density/Absorption/Void Data.....	81
Table 16: 0.54 S/B Ratio Density/Absorption/Void Data	82
Table 17: 0.58 S/B Ratio Density/Absorption/Void Data.....	83
Table 18: RCPT Data	84
Table 19: 2.5 M RMT Chloride Penetration Depth Data	85
Table 20: 5.0 M RMT Chloride Penetration Depth Data	85
Table 21: 7.5 M RMT Chloride Penetration Depth Data	86
Table 22: 10.0 M RMT Chloride Penetration Depth Data	86
Table 23: 12.5 M RMT Chloride Penetration Depth Data	86
Table 24: 2.5 M Rates of Chloride Penetration Data	87
Table 25: 5.0 M Rates of Chloride Penetration Data	87
Table 26: 7.5 M Rates of Chloride Penetration Data	88
Table 27: 10.0 M Rates of Chloride Penetration Data	88
Table 28: 12.5 M Rates of Chloride Penetration Data	89

List of Figures

Figure 1: Effect of NaOH Concentration on Flow of Mortar	22
Figure 2: Effect of Solution-to-Binder Ratio on Flow of Mortar	22
Figure 3: Effect of Curing on Compressive Strength, 2.5 M 0.50 S/B Ratio	26
Figure 4: Effect of Curing on Compressive Strength, 2.5 M 0.54 S/B Ratio	27
Figure 5: Effect of Curing on Compressive Strength, 2.5 M 0.58 S/B Ratio	27
Figure 6: Effect of Curing on Compressive Strength, 5.0 M 0.50 S/B Ratio	28
Figure 7: Effect of Curing on Compressive Strength, 5.0 M 0.54 S/B Ratio	28
Figure 8: Effect of Curing on Compressive Strength, 5.0 M 0.58 S/B Ratio	29
Figure 9: Effect of Curing on Compressive Strength, 7.5 M 0.50 S/B Ratio	29
Figure 10: Effect of Curing on Compressive Strength, 7.5 M 0.54 S/B Ratio	30
Figure 11: Effect of Curing on Compressive Strength, 7.5 M 0.58 S/B Ratio	30
Figure 12: Effect of Curing on Compressive Strength, 10.0 M 0.50 S/B Ratio	31
Figure 13: Effect of Curing on Compressive Strength, 10.0 M 0.54 S/B Ratio	31
Figure 14: Effect of Curing on Compressive Strength, 10.0 M 0.58 S/B Ratio	32
Figure 15: Effect of Curing on Compressive Strength, 12.5 M 0.54 S/B Ratio	32
Figure 16: Effect of Curing on Compressive Strength, 12.5 M 0.58 S/B Ratio	33
Figure 17: Effect of NaOH Concentration on Compressive Strength, 0.50 S/B Ratio Exposed Curing	36
Figure 18: Effect of NaOH Concentration on Compressive Strength, 0.54 S/B Ratio Exposed Curing	36
Figure 19: Effect of NaOH Concentration on Compressive Strength, 0.58 S/B Ratio Exposed Curing	37
Figure 20: Effect of NaOH Concentration on Compressive Strength, 0.50 S/B Ratio Moisture Curing	37
Figure 21: Effect of NaOH Concentration on Compressive Strength, 0.54 S/B Ratio Moisture Curing	38
Figure 22: Effect of NaOH Concentration on Compressive Strength, 0.58 S/B Ratio Moisture Curing	38
Figure 23: Effect of NaOH Concentration on Compressive Strength, 0.50 S/B Ratio Sealed Curing	39
Figure 24: Effect of NaOH Concentration on Compressive Strength, 0.54 S/B Ratio Sealed Curing	39
Figure 25: Effect of NaOH Concentration on Compressive Strength, 0.58 S/B Ratio Sealed Curing	40
Figure 26: Effect of Solution-to-Binder Ratio on Compressive Strength, 2.5 M Exposed Curing	44
Figure 27: Effect of Solution-to-Binder Ratio on Compressive Strength, 2.5 M Moisture Curing	44
Figure 28: Effect of Solution-to-Binder Ratio on Compressive Strength, 2.5 M Sealed Curing	45
Figure 29: Effect of Solution-to-Binder Ratio on Compressive Strength, 5.0 M Exposed Curing	45
Figure 30: Effect of Solution-to-Binder Ratio on Compressive Strength, 5.0 M Moisture Curing	46
Figure 31: Effect of Solution-to-Binder Ratio on Compressive Strength, 5.0 M Sealed Curing	46
Figure 32: Effect of Solution-to-Binder Ratio on Compressive Strength, 7.5 M Exposed Curing	47

Figure 33: Effect of Solution-to-Binder Ratio on Compressive Strength, 7.5 M Moisture Curing	47
Figure 34: Effect of Solution-to-Binder Ratio on Compressive Strength, 7.5 M Sealed Curing	48
Figure 35: Effect of Solution-to-Binder Ratio on Compressive Strength, 10.0 M Exposed Curing	48
Figure 36: Effect of Solution-to-Binder Ratio on Compressive Strength, 10.0 M Moisture Curing	49
Figure 37: Effect of Solution-to-Binder Ratio on Compressive Strength, 10.0 M Sealed Curing	49
Figure 38: Effect of Solution-to-Binder Ratio on Compressive Strength, 12.5 M Exposed Curing	50
Figure 39: Effect of Solution-to-Binder Ratio on Compressive Strength, 12.5 M Moisture Curing	50
Figure 40: Effect of Solution-to-Binder Ratio on Compressive Strength, 12.5 M Sealed Curing	51
Figure 41: Effect of NaOH Concentration on 7-Day Void Content	59
Figure 42: Effect of Solution-to-Binder Ratio on 7-Day Void Content	59
Figure 43: Effect of NaOH Concentration on 7-Day RMT Migration Coefficient	66
Figure 44: Effect of Solution-to-Binder Ratio on 7-Day RMT Migration Coefficient	66

Introduction

Concrete is the predominant material used for construction, with over 7 billion tons produced each year. Ordinary Portland cement (OPC) is the main binding material used in concrete. OPC production accounts for a significant amount of CO₂ emissions, raising an issue regarding the sustainability of the construction industry. Another concern is the inability of OPC to maintain physico-chemical long-term durability in adverse environmental and climatic conditions. Current research has shown that alkali-activated natural pozzolans may be able to address these two concerns. What follows is a literature review summarizing the sustainability and durability of OPC and alkali-activated natural pozzolans, the background of pozzolanic materials, and previous studies dealing with the activation of natural pozzolans. The need for future research into alkali-activated natural pozzolans is also described.

1. Literature Review

1.1 Sustainability

Huntzinger and Eatmon (2009) [1] addressed the life-cycle assessment of OPC manufacturing. Concrete is the most widely used man-made construction material with approximately 1 ton produced per person every year [1]. OPC production accounts for nearly 5% of the world's total CO₂ emissions, with half of the CO₂ emissions produced as calcium carbonate (CaCO₃) is transformed to calcium oxide (CaO) in the kiln and the other half of the emissions resulting from energy usage [1]. The OPC production process is energy intensive because it requires treating the raw materials in a kiln at temperatures greater than 1400°C [1]. Similarly, Roy (1999) [2] found that concrete is the most widely produced manufactured material

by volume in the world. Its use has contributed a sizeable amount of CO₂ to the atmosphere due to the high-energy demand of OPC production to heat the kiln as well as creating CO₂ as a by-product of the decarbonation of limestone.

Equation 1: Decarbonation of Limestone



Pacheco-Torgal et al. (2012) [3] provided another assessment of the global CO₂ emissions due to OPC production, finding an estimate around 7%. In the next forty years, the predicted demand for OPC will double, reaching 6 billion tons per year [3]. Given this growth rate, the replacement of OPC with alkali-activated binders may significantly reduce the amount of CO₂ emitted into the atmosphere. In the view of this research, the term “sustainable” refers to the preservation of the environment through the reduction of CO₂ emitted into the atmosphere due to OPC production. Additionally, natural pozzolans are not only a sustainable option for an OPC replacement, but they also offer economic benefits. Using natural pozzolans can save contractors up to 25% when compared to using OPC due to reduced material expenses during the production process [1].

1.2 Durability

Pacheco-Torgal et al. (2008) [4] discussed the limitations of OPC in terms of durability. One study found that 40% of the 600,000 bridges in the United States are affected by corrosion problems, summing up to a total cost of \$50 billion in repairs [4]. These bridges are constructed from OPC, thus suggesting that finding an alternative binder with improved permeability

resistance could substantially reduce future construction repair costs. Research into alkali-activated binders as a replacement of OPC has shown favorable results with respect to durability. Alkali-activated binders have the potential to provide multiple benefits including increased chemical resistance, increased freeze-thaw resistance, and greater stability in high temperatures [3].

Another aspect of durability under question is why the 2000-year old ancient Greek and Roman concrete structures have been able to resist decay while the structures of today display a need for repair after only a decade of use. Jackson et al. [5] studied these Ancient Roman monuments and found that they consisted of brick and volcanic tuff clasts bonded together by pozzolan mortars. The pozzolan used during this time period was the alkali-rich Pozzolane Rosse ash, which has proven extremely durable over millennia [5]. This indicates that alkali-activated pozzolanic materials may prove to be a viable solution to modern concrete durability concerns.

1.3 History of Pozzolanic Materials

Ancient mortars were made from both alkali-rich volcanic ash aggregate and calcium-alumina-silicate hydrate cements [5]. The ACI Committee 232 (2001) [6] reported that the first examples of pozzolanic binders were found near the Persian Gulf, dating back to 5000-4000 B.C. and consisting of a mixture of lime and natural pozzolan. The Greeks began using lime-pozzolan mixtures around 700 B.C., and the Romans followed them in 150 B.C. [6]. In the 2nd century B.C., Roman builders began experimenting with various concrete materials, and by the Augustan Era (27 B.C. to A.D. 14), builders identified the Pozzolane Rosse ignimbrite ash aggregate as one of the most suitable in terms of strength and durability [5]. This alkali-containing ash

produced calcium-silicate hydrate (CSH) gel cements, indicating a strong reaction between this ash and the hydrated lime [5].

Studies of ancient concrete structures in Italy, Greece, Cyprus, and Egypt found that these concretes have survived corrosive conditions for over 2000 years whereas Portland cement exposed to the same environment needed to be repaired after 10 years [2]. The long-term durability of these structures indicated that the reactions between the ash and hydrated lime might have increased the sorption and binding of the materials [5]. Winter explains that the alkali-silica reaction in pozzolanic materials occurs when the materials are initially mixed, causing no expansion [7]. In contrast, OPC is typically used with low alkali aggregates due to an increased likelihood of failure and cracking [5]. Alkali aggregates in concrete made with OPC experience alkali-silica reactions. This reaction with calcium to produce CSH gel occurs after the concrete has been cured, leading to expansion and crack formation within the concrete [7].

1.4 Chemistry of Pozzolanic Materials

Pozzolans are defined as inorganic materials containing aluminates and silicates that form hydrates when mixed with lime and water [5]. Research into alkali-activated cements began in the 1940s predominantly with the work of Glukhovsky who focused on explaining the difference between the compositions of OPC and other minerals found in the earth's crust [2]. He found that OPC forms calcium silicate hydrate (CSH) and portlandite ($\text{Ca}(\text{OH})_2$) as hydration products, whereas the other minerals predominantly form zeolites, also called aluminum silicate hydrates, that lead to enhanced durability [2]. Glukhovsky (1959) [8] also investigated the binders used in ancient Roman and Egyptian structures. He found that these ancient concretes were made of aluminosilicate calcium hydrates, similar to the ones in OPC, but they also contained a natural

mineral called analcite [8]. Glukhovsky called these binders “soil-cement” and they were produced from aluminosilicate mixed with alkali-rich industrial wastes [8].

Khale and Chaudhary (2007) [9] explain that OPC is classified as a cementitious material, having a calcium oxide (CaO) to total mass ratio greater than 20%. Kosmatka et al. (2002) [10] say this allows hydration of OPC to occur naturally as the tricalcium silicate ($3\text{CaO}\cdot\text{SiO}_2$) and dicalcium silicate ($2\text{CaO}\cdot\text{SiO}_2$) interact with water to form calcium hydroxide (CaOH) and CSH. For pozzolans, materials with a CaO to total mass ratio less than 20%, hydration does not occur naturally; there needs to be some catalyst to begin the reaction since these materials are not cementitious on their own [4]. Alkali-activators, such as sodium hydroxide (NaOH), are used to initiate the reaction.

Glukhovsky et al. (1980) [11] identified the reaction mechanism for alkali-activated binders as consisting of the breakdown of covalent Si-O-Si and Al-O-Si bonds when the pH increases, transforming these groups into a colloidal phase. The destroyed products then accumulate into a coagulated arrangement, thus generating a condensed structure [11]. Other authors are in agreement with Glukhovsky that the activation process consists of three phases: silica dissolution, transportation, and polycondensation. Purdon (1940) [12] also worked with slag and sodium hydroxide in the 1940s. He found that the activation process occurred in two steps: silica aluminum and calcium hydroxide were liberated and then silica and alumina hydrates were formed as the alkali solution was regenerated [12]. Although the number of steps of the alkali-activator and pozzolan reaction is debatable, it is evident that the alkali-activator is essential to breaking down silica and aluminum bonds so that hydrates can form.

Alkali concentration plays a significant role in the geopolymerization process. As the hydroxide ion concentration is increased, there is also an increase in aluminosilicate solubility,

leading to an increase in compressive strength [9]. As more aluminosilicate bonds are broken down, there are further opportunities for hydrates to be formed that account for the majority of the mixture's strength. As the silica content available for reaction increases, there is more alkali aluminosilicate gel formed, leading to increased compressive strengths [9]. Furthermore, under hydrothermal curing, higher temperatures lead to the formation of more aluminosilicate gel [13]. This produces a molecular structure with improved orientation that enhances strength properties [13].

1.5 Effect of Temperature

In addition to alkali concentration, temperature is another contributing factor to pozzolan strength development. Unlike OPC that achieves high compressive strengths when cured in high humidity environments, pozzolans do not perform well when cured at high humidity and ambient temperatures [9]. Instead, research shows that curing in the temperature range of 30°C to 90°C has a positive effect on the pozzolan's strength characteristics [9]. Lemougna et al. (2011) [14] found that compressive strength increases as the curing temperature increases from 40°C to 90°C. Additionally, Lemougna et al. found that in this temperature range, samples cured for 7 days in dry conditions achieved significantly higher compressive strengths than those cured in wet conditions [14]. Bondar et al. (2011) [15] found that the temperature allows the excess water to evaporate, forming a monolithic geopolymer that is able to achieve full strength as the network of hydrates develop. Bondar et al. report that mixtures with a higher viscosity due to increased alkali concentration may need longer curing times and/or higher temperatures to remove this water to allow for proper bonding [15].

Research has shown that curing pozzolanic mixtures at ambient temperatures does not allow for adequate strength development because the beginning of setting is delayed [9]. This was remedied by short-term curing at 75°C for four hours with no further high temperature curing, ultimately achieving desired strength performance [9]. Khale and Chaudhary further state that the strength development did not significantly improve after 48 hours of elevated temperature curing [9]. In fact, curing at increased temperatures for longer periods of time may cause compressive strength to decrease as the gel dehydrates and begins to shrink, breaking the mixture's granular structure [9].

Lemougna et al. further studied of the effect of heat on geopolymers by exposing samples to temperatures up to 900°C. At 90°C, the highest compressive strength was achieved; however, beyond that temperature, the compressive strength significantly decreased [14]. As the temperature rose to 250°C, the strength was nearly halved as a result of the loss of structural water [14]. This severely weakened the structural geopolymer matrix as well as contributed to the formation of micro cracks [14]. The strength remained constant until 750°C at which the strength began to slightly increase as the temperature rose to 900°C [14].

1.6 Mechanical Strength

Bondar et al. conducted the majority of the experimental research into the alkali-activation of natural pozzolans. Bondar et al. (2011) [15] found that KOH added to natural pozzolans in concentrations of 5-7.5 M produced the highest compressive strength mortar after 28 days of curing. Additionally, Bondar et al. (2011) [16] tested the mechanical strength, consisting of the compressive and tensile strengths, of concrete produced with Taftan Andesite natural pozzolan at varying water to binder ratios (w/b ratio) and curing conditions. Results

revealed that the sealed curing condition produced samples with the highest compressive strengths. Furthermore, the 0.45 w/b ratio samples achieved greater compressive strengths than samples made with a 0.55 w/b ratio [16]. The splitting tensile tests showed that the short-term 28-day tensile strengths of alkali-activated natural pozzolan concrete are greater than that of the OPC control mixture at a w/b ratio of 0.45, while the converse is true at a w/b ratio of 0.55. The long-term 180-day tensile strengths of alkali-activated natural pozzolan concrete are larger than those of OPC control mixes at both w/b ratios. The 0.45 w/b ratio samples achieved greater tensile strengths at both ages of testing than the 0.55 w/b ratio samples. Additionally, the alkali-activated natural pozzolan concretes showed less drying shrinkage than that of the normal Portland cement concrete at the same w/b ratios.

In summary, the mechanical strength results show that natural pozzolans are able to act as a potential replacement for OPC with alkali activation. Most of the samples tested were able to exceed the required compressive strength for structural concrete, 3000 psi or 20.7 MPa. Additionally, these results indicate the role of the natural pozzolan's chemical composition on the achieved mechanical strength. The natural pozzolans had chemical compositions that only varied by a couple of percent with regards to the amount of SiO_2 , Al_2O_3 , and CaO present; however, the compressive strength results showed a wide range of variation. This indicates that natural pozzolans coming from different sources will have unique reactions upon activation, so each source should be tested to determine which alkali activator, concentration, and heat treatment is best suited to reach desired results.

1.7 Transport Properties

Bondar et al. also studied the transport properties, such as the oxygen and chloride permeability, of concrete made with natural pozzolans [17]. The results showed that the natural pozzolans had an oxygen permeability 10-35% lower than that of similar OPC samples tested at 90 days. Additionally, oxygen permeability was reduced as the w/b was reduced. Overall, alkali-activated natural pozzolan concrete has increased resistance to oxygen permeability when compared to OPC concrete.

In addition to oxygen permeability, the concrete samples were also tested for chloride permeability using two methods. The rapid chloride penetration test (RCPT) was used to measure the short-term chloride permeability of the samples. RCPT results revealed that the chloride permeability increased with higher w/b ratios [17]. The second method used to measure chloride permeability was the bulk diffusion test. This specifically measures the long-term chloride permeability, testing samples after one side of the sealed sample has been exposed to a 2.8 M NaCl solution for 90 days. These results show that the percentage of chloride ion penetration was generally lower in samples with lower w/b due to the tighter pore structure [17].

The transport property results show that alkali-activated natural pozzolans do have potential to increase the durability of concrete mixtures in comparison to OPC. The natural pozzolans were able to achieve significantly lower oxygen permeability values than OPC. Additionally, chloride permeability is affected by the w/b ratio, with a lower ratio having a lower percentage of chloride ion penetration. When compared to OPC concrete, alkali-activated natural pozzolan concrete was shown to have lower chloride permeability in higher strength mixtures achieving a compressive strength greater than 33 MPa.

2. Research Objectives

To address the modern concern of global climate change, ways to reduce the worldwide CO₂ emissions must be studied. One way to lessen these emissions within the construction industry is to find a new binder that can replace OPC without compromising concrete's properties. Studies have indicated that natural pozzolans activated with alkalis show promise as a substitute for OPC because they reduce the environmental impacts, lower overall costs, and achieve higher durability than concrete produced solely with OPC. However the literature is limited in this area and comprehensive studies are required. This study focused on the properties of mortars produced with alkali-activated natural pozzolans as their primary binder.

The objectives of this study included 1) activation of natural pozzolans with various alkalis to determine the optimal activation concentrations and curing conditions; 2) assessment of the strength performance of mortars made with alkali-activated natural pozzolans and 3) evaluation of the mortar's transport properties including chloride ion penetration and absorption.

3. Materials and Experimental Program

Previous investigations revealed that under suitable activation and curing conditions, production of alkali-activated natural pozzolans with superior or similar performance to that of OPC is possible. The type of activator, which can be in different concentrations and combinations of sodium hydroxide (NaOH), potassium hydroxide (KOH) and sodium silicate (Na₂SiO₃), plays an important role in the performance of these newly developed binders. The curing temperature was also found as an important factor. Accordingly, the plan for this research was to activate natural pozzolans using different activators and under different curing conditions. Mixtures were prepared using NaOH in concentrations of 2.5, 5, 7.5, 10, and 12.5 M and s/b

ratios of 0.50, 0.54, and 0.58. Each mix underwent four different curing conditions: curing room (sealed, 7 and 28 days), oven (exposed, 7 days), oven (sealed, 7 days), and oven (moisture, 7 days). The curing room samples were wrapped in plastic wrap three times and placed in a curing room at ambient temperatures with constant moisture produced by misters. The rest of the samples were cured in an oven maintained at 80°C. The exposed curing samples were placed directly on the oven racks, completely exposed to the oven environment. The sealed curing samples were wrapped three times in plastic to retain moisture within the sample and then placed on the oven racks. The moisture curing samples were placed on a rack inside of a turkey pot that had 1-2 inches of water contained beneath the rack the samples rested on. This water was maintained at a constant level throughout the testing period.

3.1 Materials

Natural pozzolans obtained from the Nevada Cement Company in Fernley, Nevada were used for all mixtures in this study. These pozzolans were selected because they come from the closest source of natural pozzolans in relation to the university where the study was performed. The chemical composition of the natural pozzolans was analyzed by Francis and is reported in Table 1 [18].

Table 1: Chemical Composition (oxide percent) of the Materials Used in this Study

Natural Pozzolan	
LOI	3.7
SiO₂	68.8
Al₂O₃	8.5
Fe₂O₃	1.1
CaO	3.2
SO₃	0.1
K₂O	3.9
Na₂O	2.6

The natural pozzolan has a total silica, aluminum, and iron content of 78.4%. The calcium oxide content (3.2%) is low, indicating that this material is not cementitious on its own. The particle size is such that 9.4% is retained on the 325 (45 μm), indicating the fineness of the natural pozzolans.

The mortar samples incorporated fine aggregates from Aggregate Industries, Inc. from Sloan, Nevada. The sieve analysis was performed by Concrete-Material Consultants, LLC and is shown in Table 2 [19]. The aggregate had an oven-dry specific gravity of 2.755 and absorption of 0.81. The aggregate was added in a fine aggregate-to-binder ratio of 2:1 ratio. Samples were prepared with a Hobart AS 200T industrial mixer.

Table 2: Amount Finer Than Each Laboratory Sieve, Mass Percent

Sieve Size	Results
3/8 in.	100
#4	100
#8	95
#16	65
#30	43
#50	24
#100	9
#200	2.7
Fineness Modulus	2.64

NaOH pellets from Duda Energy were dissolved in distilled water to create the alkali-activating NaOH solution in concentrations of 2.5, 5.0, 7.5, 10.0, and 12.5 M.

3.2 Mortar Preparation

Mortar samples were prepared by adding one-half of the NaOH solution in the mixing bowl of the Hobart AS 200T industrial mixer, followed by carefully adding in the natural pozzolans and sand. It was found that adding the NaOH solution first allowed for easier and more thorough mixing. The sand, natural pozzolans, and NaOH solution were mixed for two minutes on the slow speed. The remaining one-half of the NaOH solution was added and the mortar was mixed on the slow speed for an additional two minutes. To ensure that all of the natural pozzolans had been exposed to the NaOH solution, hand mixing was incorporated for a minute. Additional water was then added and the mortar was mixed on the medium speed for thirty seconds. The mortar was checked to ensure that mixing was complete. If needed, additional hand mixing was incorporated.

3.3 Flow

The flow of each sample was measured according to ASTM C1437 [22] to determine the differences in the fresh properties of the mortars. The test procedure was as follows:

- a. Immediately after mixing, mortar was placed into the flow mold to an approximate height of 1 inch.
- b. The mortar was tamped 20 times with tamper.
- c. The remaining volume of the flow mold was loaded with a second layer of mortar.
- d. This layer was tamped 20 times and then made flush with the surface of the mold.
- e. The mold was lifted away from the mortar followed by immediately dropping the flow table 25 times in 15 seconds.
- f. The diameter of the mortar on the flow table was measured three times to achieve an average value indicating the amount of flow.

3.4 Compressive and Flexural Strengths

The compressive test is an indication of the concrete's strength. Compressive tests were performed on 2-inch cube samples in a procedure similar to ASTM C109 using a Tinius Olsen testing machine [21]. Four samples of each mixture were tested in a compressive machine by applying a constant load until the cube cracked and experienced failure. The load was applied at a 0.05 in/min. loading rate. The load at failure was divided by the area of the cube's face to determine the compressive strength. The following equation was used:

Equation 2: Compressive Strength

$$fm = \frac{P}{A}$$

where:

f_m = compressive strength in MPa or [psi]

P = total maximum load in N or [lbf]

A = area of loaded surface mm^2 or [in^2]

The flexural test determined the flexural strength of a beam experiencing a load. The result is reported as the modulus of rupture. The test was performed in accordance with ASTM C78 [20] for a simple beam using third-point loading. Beams were made for each sample and cured in the oven at 80°C for 7 days prior to testing. Four beams were tested for each sample. One beam in each mixture had a 1-inch Vishay Precision Group strain gage attached to it according to Vishay's application note TT-611 for strain gage installations for concrete structures to measure the strain experienced by the beam under loading. The load was applied continuously by the compressive machine at a rate of 0.03 in/min. until the beam was fractured and unable to support any load. The modulus of rupture was calculated using the following equation:

Equation 3: Modulus of Rupture

$$R = \frac{PL}{bd^2}$$

where:

R = modulus of rupture in MPa or [in]

P = maximum applied load indicated by the testing machine in N or [lbf]

L = span length in mm or [in.]

b = average width of specimen at the fracture in mm or [in.]

d = average depth of specimen at the fracture in mm or [in.]

3.5 Density/Absorption/Voids

The absorption test provided an indication of the mortar's ability to take in water. The testing procedure followed ASTM C642 [23] and used a balance sensitive to 0.025% of the specimen's mass. Samples were tested for each mixture after 7 days of sealed curing in the oven and 28 days in the curing room. The test was performed according to the procedure below:

- a. The original mass was reported as X.
- b. The sample was dried in an oven at 100-110°C for at least 24 hours and then removed to measure the mass. The sample was considered dry when the difference between the two successive masses was less than 0.5% of the lesser value. The dry mass was recorded as A.
- c. After drying, the sample was immersed in tap water for at least 48 hours and then the mass was measured. The sample was saturated surface-dried by removing any excess moisture from the sample with a towel. When the differences in the sample's saturated surface-dried masses were less than 0.5% of the larger value at intervals of 24 hours, the saturated surface-dried mass was recorded as B.
- d. The sample was submerged in tap water and boiled for 5 hours. After boiling, the sample was allowed to cool in tap water for not less than 14 hours to a final temperature between 20-25°C. The sample was saturated surface-dried before the mass was measured. This soaked, boiled, and surface-dried mass was recorded as C.
- e. After immersion and boiling, the mass was suspended by a wire to determine the apparent mass in water. This was denoted as D.
- f. The absorption after immersion was found using the following equation:

Equation 4: Absorption After Immersion

$$\% = \frac{B - A}{A} \times 100$$

- g. The absorption after immersion and boiling was determined by:

Equation 5: Absorption After Immersion and Boiling

$$\% = \frac{C - A}{A} \times 100$$

- h. The dry bulk density was calculated as follows and was denoted by g_1 :

Equation 6: Dry Bulk Density

$$g_1 = \frac{A}{C - D} \times \rho$$

Note: $\rho = 1\text{g/cm}^3$

- i. The bulk density after immersion was found using the following equation:

Equation 7: Bulk Density After Immersion

$$= \frac{B}{C - D} \times \rho$$

- j. The bulk density after immersion and boiling was found as follows:

Equation 8: Bulk Density After Immersion and Boiling

$$= \frac{C}{C - D} \times \rho$$

- k. The apparent density was determined using the following equation and was denoted as g_2 .

Equation 9: Apparent Density

$$g_2 = \frac{A}{A - D} \times \rho$$

- l. The volume of permeable pore space, otherwise known as the voids, was found as follows:

Equation 10: Volume of Permeable Pore Space

$$\% = \frac{g_2 - g_1}{g_2} \times 100$$

3.6 Rapid Chloride Penetration Test

The rapid chloride penetration test (RCPT) was used to determine the electrical conductance of concrete that indicates the concrete's ability to resist chloride ion penetration. This test followed the standards set forth by ASTM C 1202 [24] "Electrical Indication of Concrete's Ability to Resist Chloride Ion Penetration". A vacuum desiccator, pump, specimen-cell sealant, beaker, power supply, and distilled water were used to complete the test. The mortar samples were cast in 100 mm (4 in.) diameter and 50 mm (2 in.) height molds. The test procedure was as follows:

- a. The specimens were air dried for at least 1 hour and the sides were coated with a plastic dip and allowed to dry.
- b. The specimens were placed in the desiccator with the pump operating for 3 hours. The pressure of the desiccator was maintained at less than 1 mm Hg (133 Pa).
- c. Distilled water was added to the desiccator with the pump running. Water was added in the desiccator until the specimens were fully immersed.
- d. The pump ran for an additional hour.
- e. The pump was turned off and air was allowed to re-enter the desiccator. The specimens were left in the desiccator for 18 ± 2 hours.
- f. The specimens were removed and any excess water was wiped off. The specimens were placed in the cells with rubber gaskets to maintain the specimens at a relative humidity of 95% or higher.

- g. The testing cells were filled with either a 3.0% NaCl solution (side connected to negative terminal of power supply) or a 0.3 M NaOH solution (side connected to positive terminal of the power supply).
- h. Lead wires were attached to the cell banana posts. The computer program “Proove-It” was used at 60.0 volts initially with a testing time of 6 hours. If 60 volts caused the program to overload, the voltage was reduced to 10 volts. The initial current reading was recorded.
- i. After 6 hours, the equipment calculated the charge passed through the mortar samples.

3.7 Rapid Migration Test

The rapid migration test (RMT) was also used to provide information about the concrete’s ability to resist chloride ion penetration. This test followed the standards set forth by NT Build 492 “Chloride Migration Coefficient from Non-Steady-State Migration Experiments” [25]. The equipment used to perform this test was a vacuum desiccator, a pump, beaker, splitting device, ruler, and a migration apparatus. The migration apparatus consisted of a silicone rubber sleeve, clamp, catholyte reservoir, plastic support, cathode, and anode. Reagents included calcium hydroxide, sodium chloride, sodium hydroxide, and silver nitrate. The test specimens were 100 mm (4 in.) in diameter and 50 mm (2 in.) in height. The RMT procedure consisted of the following steps:

- a. The mortar specimens were air dried and then placed in the desiccator with the pump operating for 3 hours. The pressure of the desiccator was maintained at 1-5 kPa.

- b. After 3 hours, a calcium hydroxide solution was allowed to enter the desiccator while the pump was still running. The solution completely immersed the samples.
- c. The pump ran for an additional hour and then it was turned off. Air re-entered the desiccator and the samples remained submerged for 18 ± 2 hours.
- d. The specimens were removed and any remaining moisture was wiped off.
- e. The catholyte reservoir was filled with approximately 12 liters of 10% NaCl solution made with 100 grams of NaCl dissolved in 900 grams of tap water.
- f. The specimen was put inside the rubber sleeve and the clamps were applied around the specimens, securing them as tightly as possible.
- g. The specimens were placed on the plastic support in the catholyte support.
- h. The sleeve was filled with the anolyte solution (0.3 M NaOH). The anode was then placed in the anolyte solution.
- i. The cathode was connected to the negative pole and the anode to the positive pole of the power supply.
- j. The power supply was turned on to an initial voltage of 30 volts and the initial temperature and current were recorded. Based on the initial current, the voltage and the testing duration were adjusted.
- k. The final current and temperature were recorded before testing termination.
- l. After testing, the specimens were removed from the sleeves, rinsed, and wiped dry.
- m. The specimens were split in half axially and then sprayed with a 0.5 M silver nitrate solution.

- n. The solution reacted with the chloride ions and changed to a white color due to precipitate formation. This color change indicated the depth of chloride ion penetration.
- o. Seven depths of the mortar specimen's chloride ion penetration were measured using calipers.
- p. The rapid migration was measured by dividing the penetration depth by the applied voltage and test duration time in hours.

4. Results and Discussion

4.1 Fresh Properties – Flow and Density

The fresh densities of the mortars ranged from 2190 – 2525 kg/m³. The flow of mortar was affected by both the concentration of NaOH and s/b ratio. As the concentration of NaOH increased, the flow decreased. The flow was also reduced when lower s/b ratios were used in the mixture. Figures 1 and 2 show these trends.

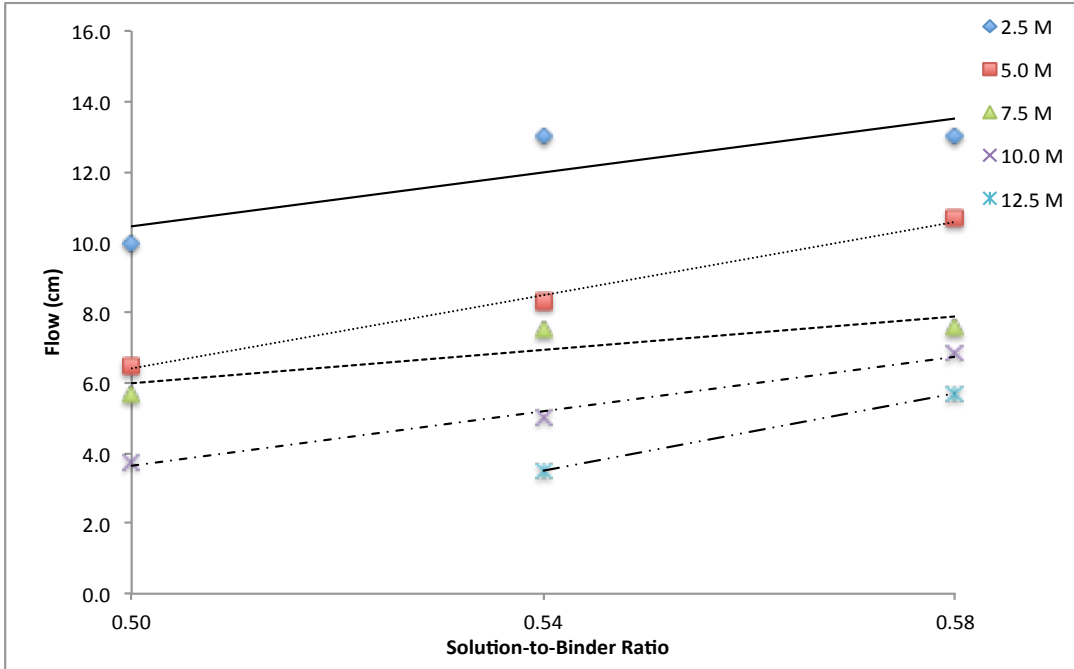


Figure 1: Effect of NaOH Concentration on Flow of Mortar

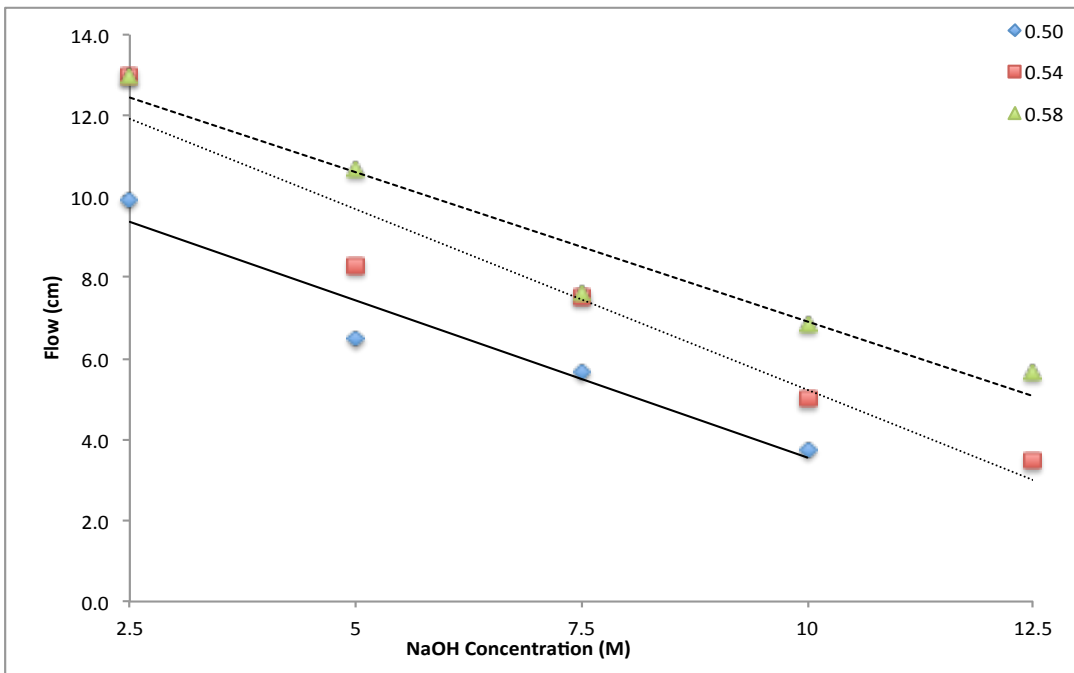


Figure 2: Effect of Solution-to-Binder Ratio on Flow of Mortar

As reported by Kosmatka et al., concrete made with OPC typically shows that when less water is added to a mixture, the concrete will become less plastic and workable, resulting in a stiffer mixture [26]. The results found for mortar made with alkali-activated natural pozzolans also followed this trend. Increasing the s/b ratio allowed for greater workability and ease of mixing.

4.2 Compressive Strength

The average compressive strengths are reported in Table 3. Fourteen mixtures were prepared and cured in three different curing conditions: exposed, moisture, and sealed. Within each curing environment, three different s/b ratios were selected for each of five NaOH concentrations. The 12.5 M 0.50 s/b ratio mixture was not used as there would not have been enough water available to create a workable mortar mixture. Compressive tests were conducted on the samples at one, three, and seven days.

Table 3: Average Compressive Strengths

S/B Ratio	NaOH Concentration	Days	Exposed (MPa)	Moisture (MPa)	Sealed (MPa)
0.50	2.5 M	1	3.775	4.159	4.584
		3	5.201	6.179	5.433
		7	4.614	9.974	5.869
	5.0 M	1	7.193	4.788	5.396
		3	8.995	7.466	9.680
		7	8.842	11.210	12.463
	7.5 M	1	10.441	6.638	7.387
		3	14.496	11.167	16.529
		7	15.271	17.339	20.548
	10.0 M	1	13.550	8.686	9.444
		3	27.687	15.926	22.267
		7	26.169	22.866	31.913
0.54	2.5 M	1	3.545	4.226	4.499
		3	4.981	5.886	5.691
		7	4.573	9.513	5.749
	5.0 M	1	6.043	4.111	4.361
		3	6.637	6.826	8.428
		7	6.802	10.476	11.372
	7.5 M	1	9.806	5.320	5.841
		3	10.986	9.235	14.751
		7	11.526	13.675	17.908
	10.0 M	1	12.797	6.706	7.894
		3	25.292	13.485	21.581
		7	24.190	21.122	28.216
	12.5 M	1	15.693	7.275	10.363
		3	30.798	16.271	24.086
		7	27.589	25.656	30.827
0.58	2.5 M	1	2.386	2.649	2.861
		3	2.961	3.879	3.394
		7	2.960	6.075	3.883
	5.0 M	1	4.738	2.450	3.018
		3	5.516	4.562	6.751
		7	5.086	6.956	8.434
	7.5 M	1	8.113	3.252	3.458
		3	10.073	6.486	12.581
		7	8.577	8.549	14.876
	10.0 M	1	11.890	4.993	5.697
		3	21.940	8.897	17.533
		7	21.579	15.003	27.095
	12.5 M	1	14.040	5.703	7.387
		3	32.386	17.354	23.310
		7	31.781	26.621	37.696

4.2.1 Effect of Curing

From Figures 3-16, it is evident that curing conditions affected the compressive strengths achieved by samples. In general, the exposed samples reached their highest compressive strengths after three days of curing. The moisture and sealed samples continuously gained strength, reaching their ultimate strengths at seven days.

After one day of curing, the 2.5 M, 5.0 M, and 7.5 M samples in the exposed curing condition gained most of their compressive strength, obtaining values ranging from 68% to 89% of their maximum strengths. These samples experienced small increases in strength from one to three days. In contrast, the 10.0 M and 12.5 M samples gained 43% to 54% of their maximum compressive strengths after one day of exposed curing. This led to a larger increase in strength between one and three days of curing. From three to seven days, most samples experienced a decrease in compressive strength.

The moisture curing samples showed a different trend than the exposed curing samples. After one day of curing, samples of all molarities achieved 21% to 44% of their ultimate strengths, indicating that moisture curing allowed for slower strength development than exposed curing. At three days, the samples reached 59% to 76% of their maximum strengths.

The sealed curing samples exhibited a trend that combined the trends shown for exposed and moisture curing conditions. The 2.5 M samples followed a trend similar to that of the exposed curing samples. They achieved most of their maximum strength (74% to 78%) after one day of curing. At three days, the samples gained strength, reaching 87% to 99% of their final strengths. The remaining 5.0 M, 7.5 M, 10.0 M, and 12.5 M samples followed a trend more

similar to that of the moisture curing samples. At one day, the samples attained 20% to 43% of their final strengths. When tested at three days, the samples gained strengths to now account for 62% to 85% of their ultimate strengths.

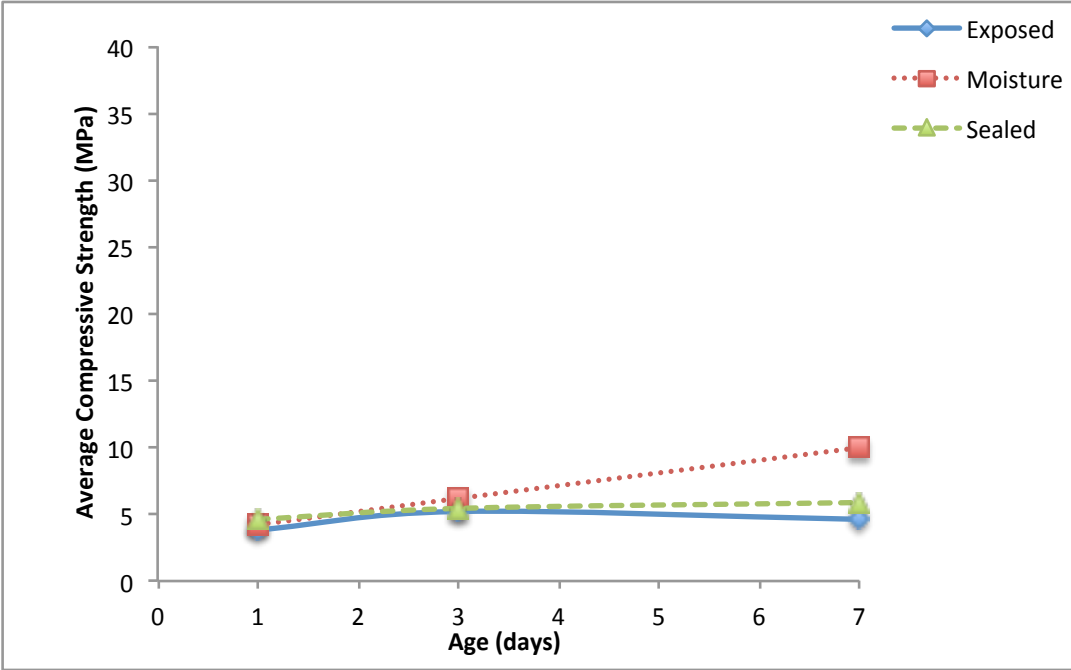


Figure 3: Effect of Curing on Compressive Strength, 2.5 M 0.50 S/B Ratio

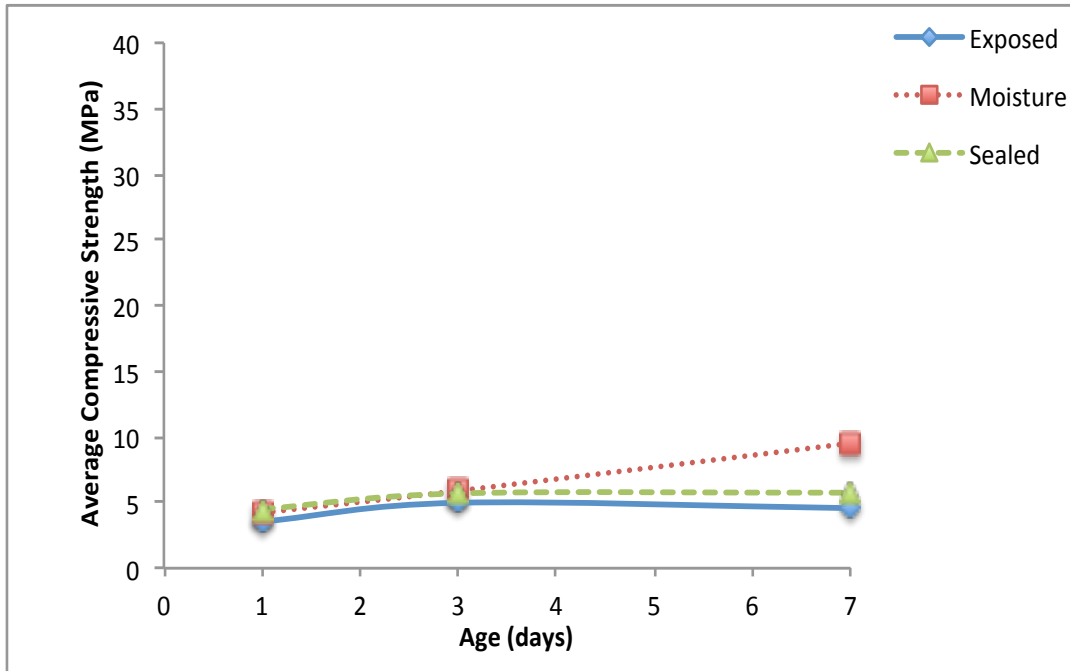


Figure 4: Effect of Curing on Compressive Strength, 2.5 M 0.54 S/B Ratio

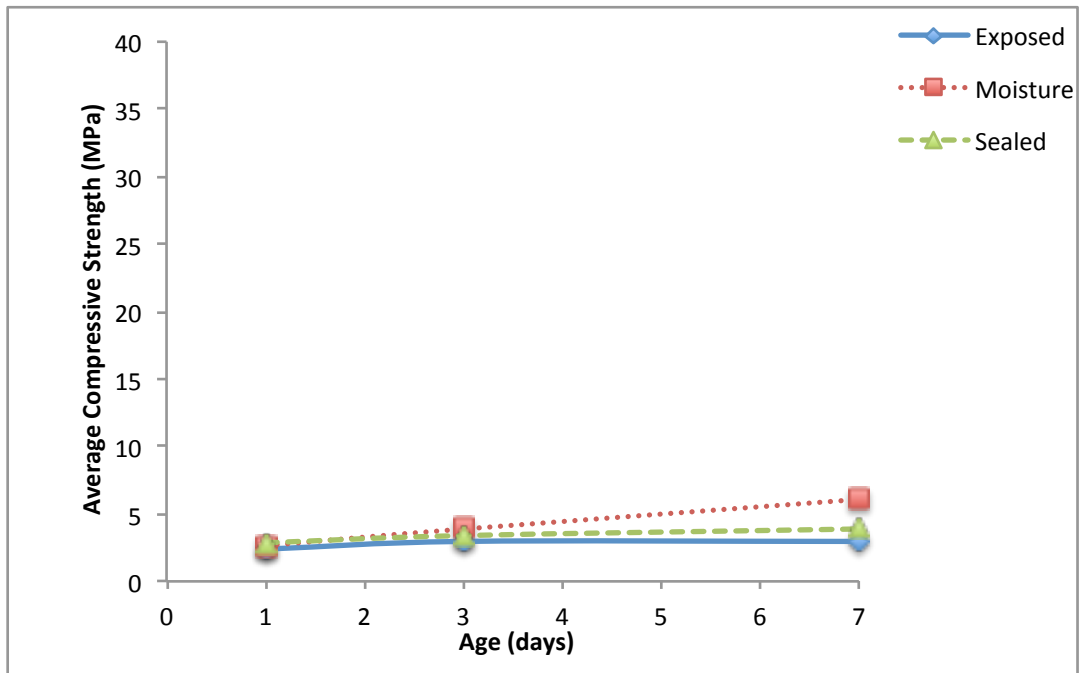


Figure 5: Effect of Curing on Compressive Strength, 2.5 M 0.58 S/B Ratio

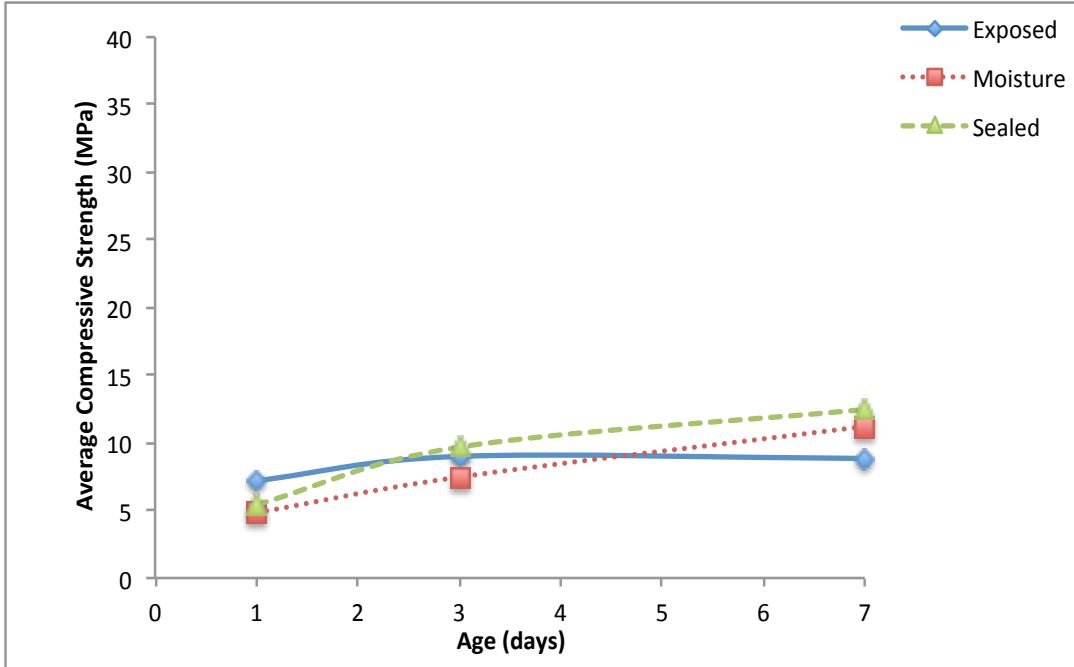


Figure 6: Effect of Curing on Compressive Strength, 5.0 M 0.50 S/B Ratio

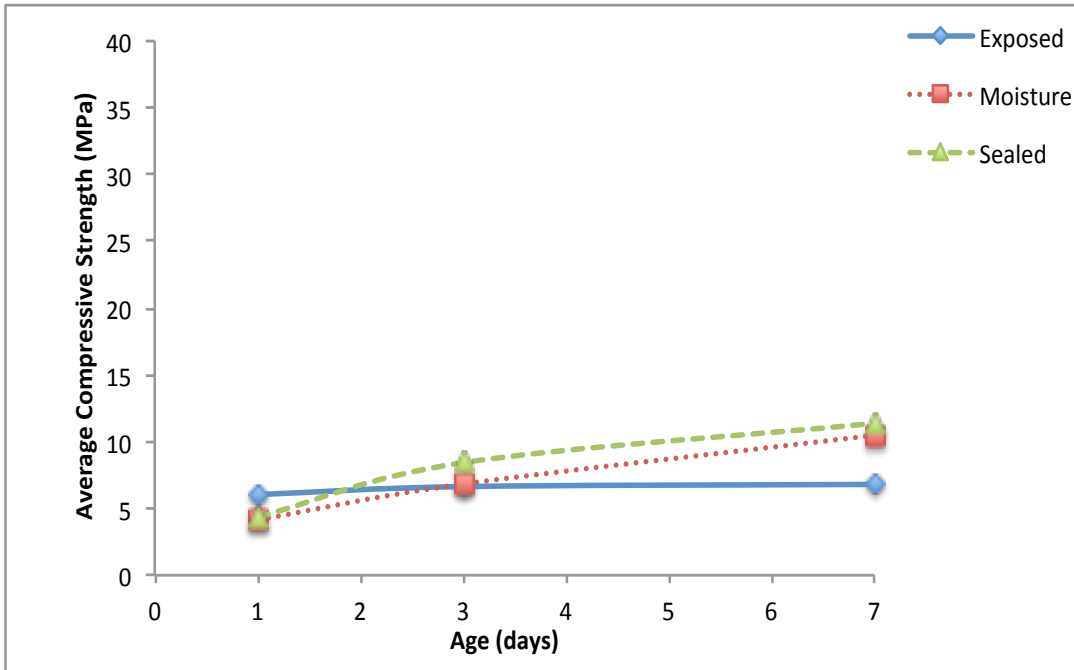


Figure 7: Effect of Curing on Compressive Strength, 5.0 M 0.54 S/B Ratio

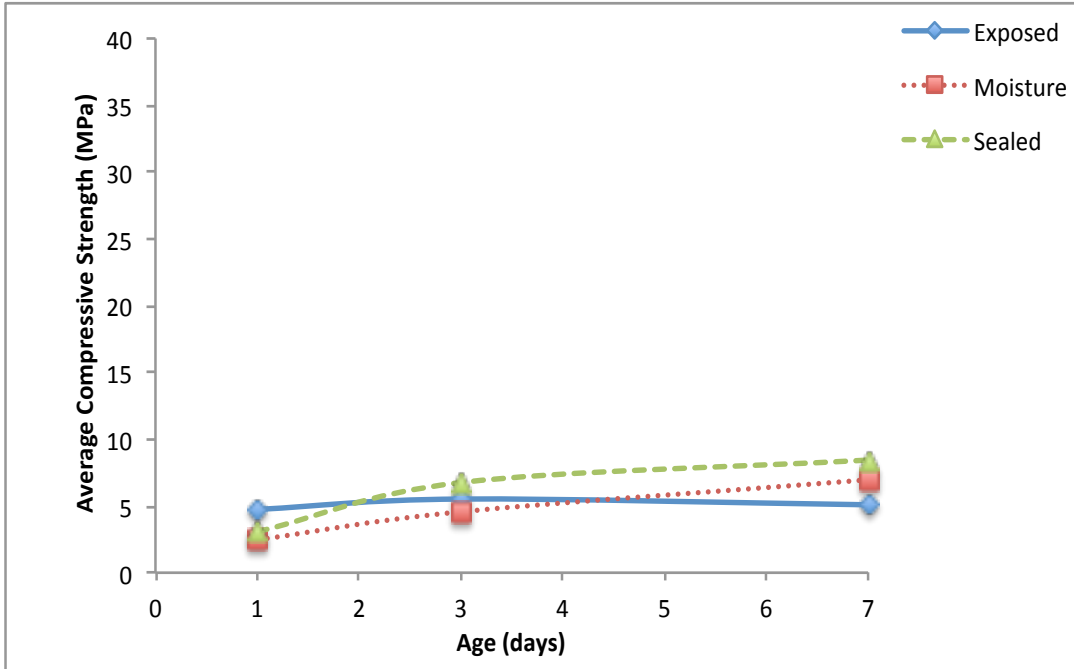


Figure 8: Effect of Curing on Compressive Strength, 5.0 M 0.58 S/B Ratio

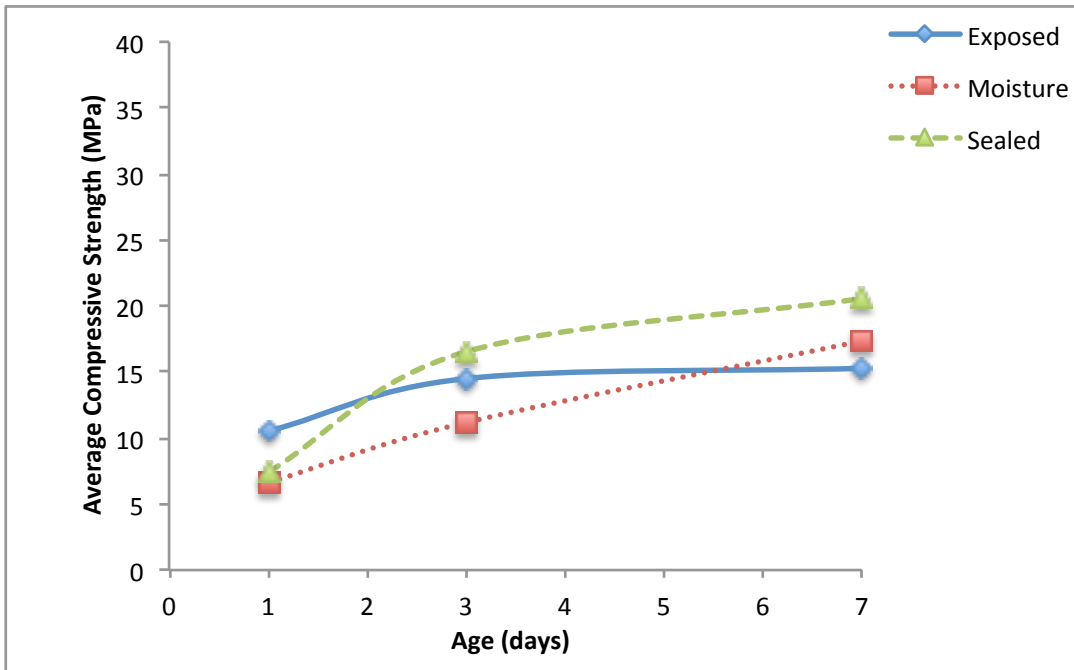


Figure 9: Effect of Curing on Compressive Strength, 7.5 M 0.50 S/B Ratio

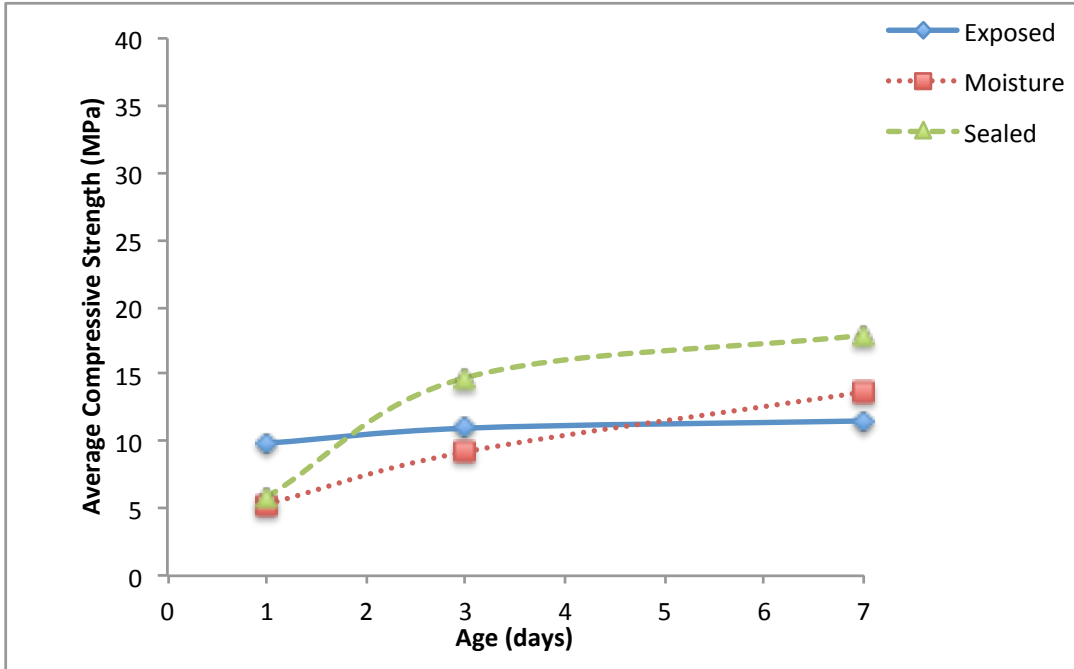


Figure 10: Effect of Curing on Compressive Strength, 7.5 M 0.54 S/B Ratio

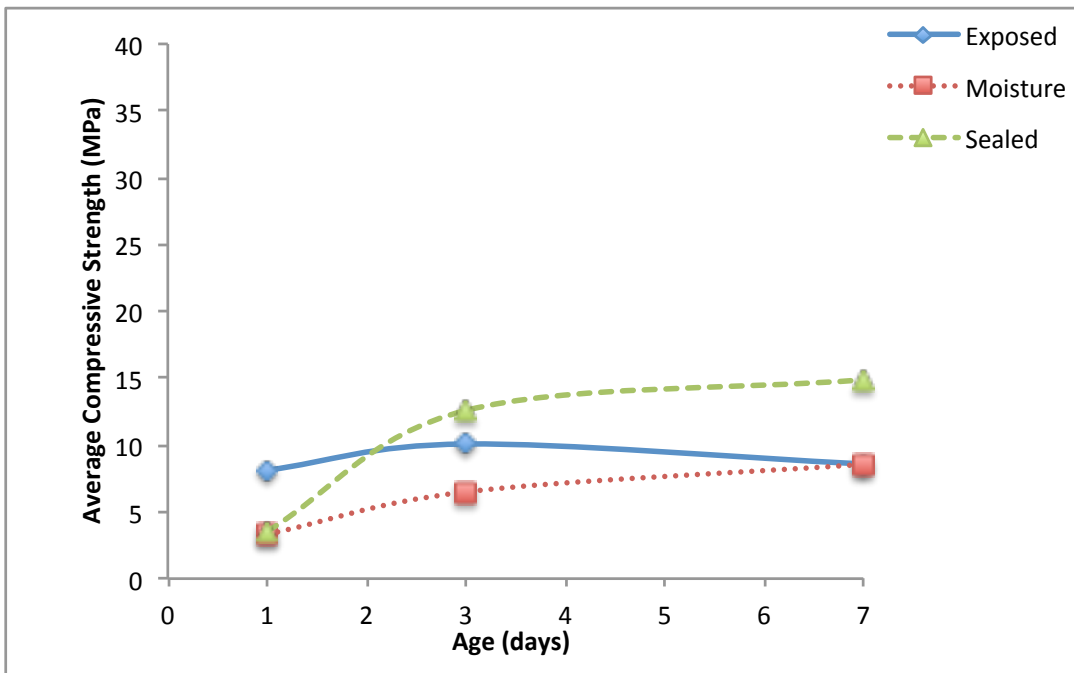


Figure 11: Effect of Curing on Compressive Strength, 7.5 M 0.58 S/B Ratio

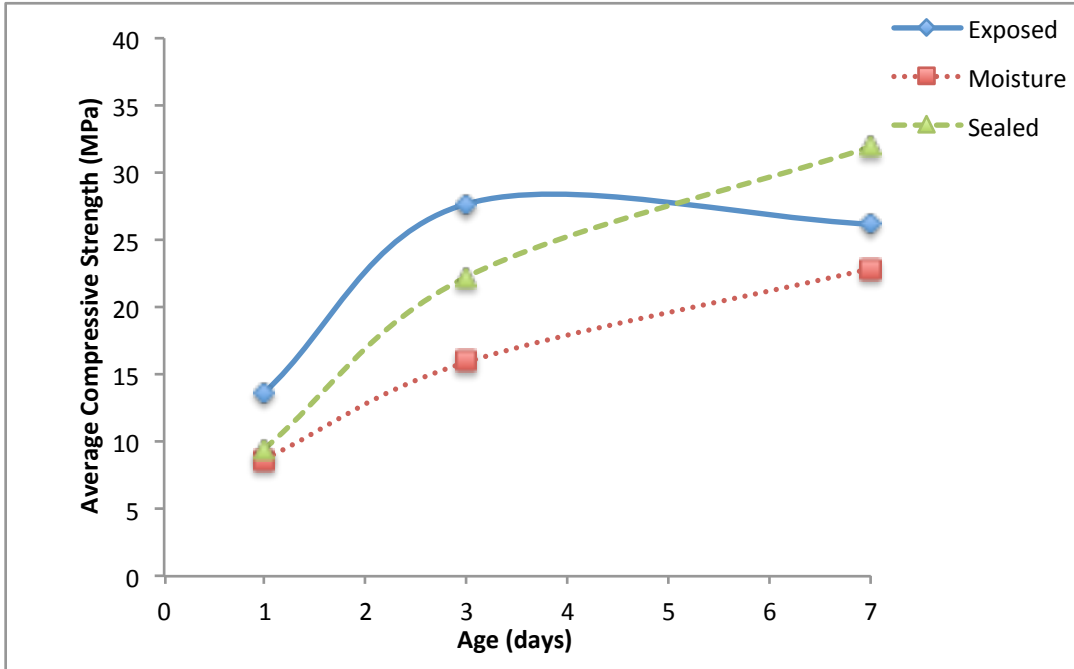


Figure 12: Effect of Curing on Compressive Strength, 10.0 M 0.50 S/B Ratio

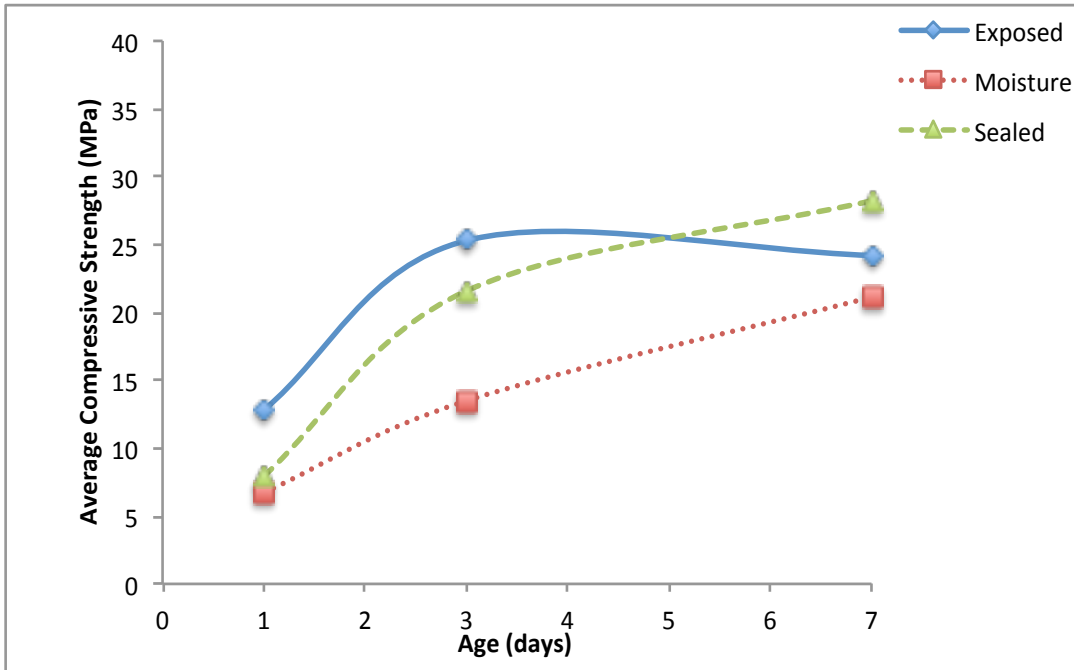


Figure 13: Effect of Curing on Compressive Strength, 10.0 M 0.54 S/B Ratio

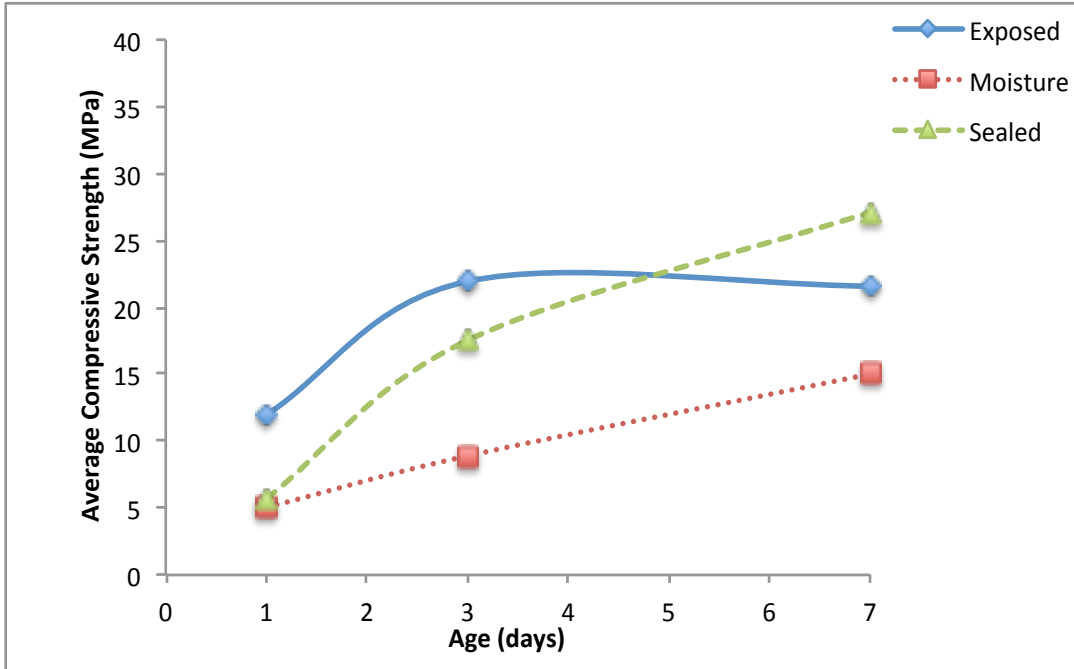


Figure 14: Effect of Curing on Compressive Strength, 10.0 M 0.58 S/B Ratio

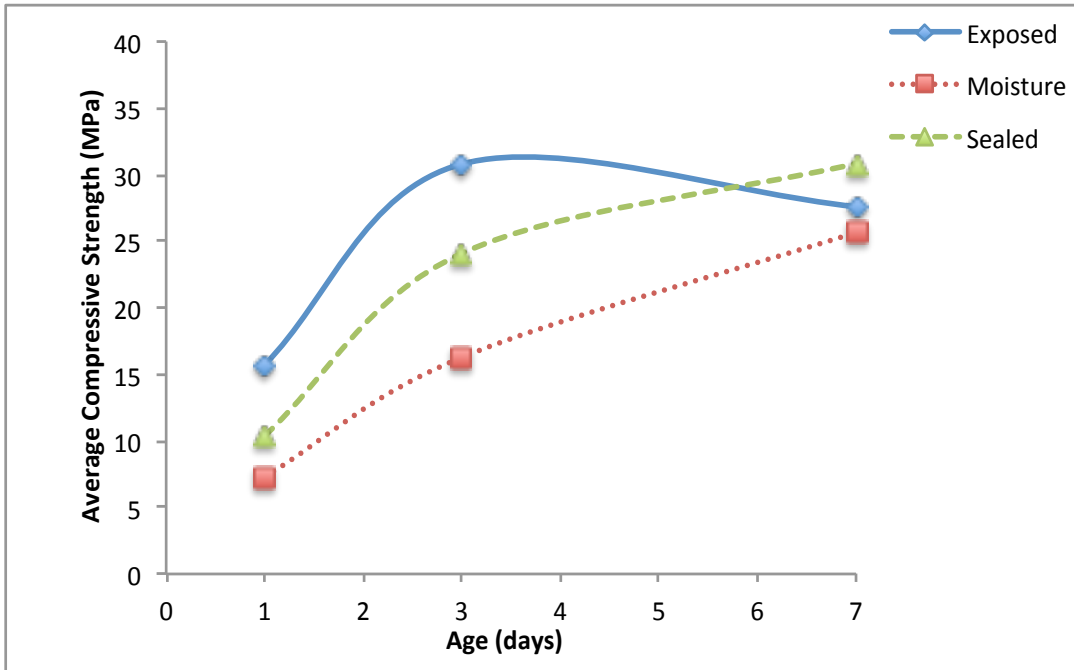


Figure 15: Effect of Curing on Compressive Strength, 12.5 M 0.54 S/B Ratio

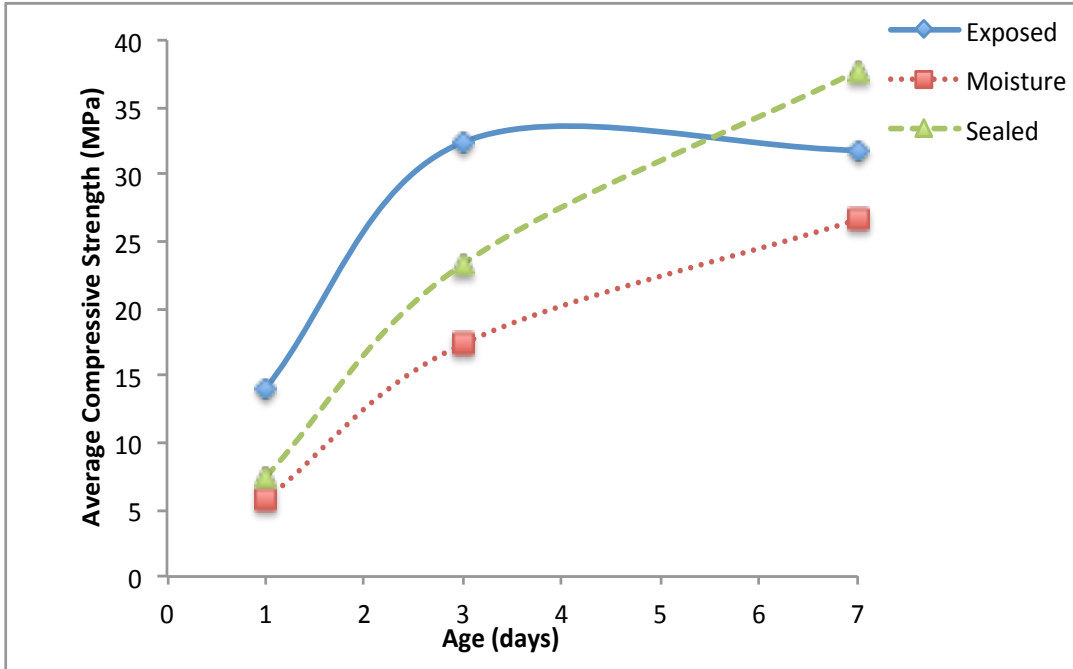


Figure 16: Effect of Curing on Compressive Strength, 12.5 M 0.58 S/B Ratio

The exposed curing condition had no humidity, allowing strength to develop quickly in all samples. The samples made with lower concentrations of NaOH (2.5 M, 5.0 M, and 7.5 M) were able to evaporate excess water after one day of curing, achieving high compressive strengths. The 10.0 M and 12.5 M samples required more time to form a monolithic geopolymer layer as these solutions had higher viscosities [15]. Therefore, at three days of curing, most exposed curing samples had attained their maximum strengths. After three days of curing, compressive strengths dropped as dehydration occurred. When samples are exposed to elevated curing temperature conditions for too long, the aluminosilicate gel begins to dehydrate and break apart, causing the samples to lose mechanical strength [9].

The exposed curing samples attained much higher strengths than the moisture curing samples. This supports previous research performed by Lemoungna et al. [14]. The moisture curing samples were cured in a high humidity environment, so the strength gain occurred at a

much slower rate. The extra water within the samples took longer to remove in a high humidity environment, causing fewer bonds to form at a slower rate.

The sealed curing samples achieved the largest overall compressive strengths. Strength development occurred at a slower rate than the exposed curing samples due to the moisture present within the samples. The plastic wrap protected the samples from the dry oven environment, allowing some moisture to be retained within the samples. In contrast to the exposed curing samples, the sealed curing samples did not experience dehydration. The samples continued to gain strength over time. This shows that in order to achieve the greatest compressive strengths, some moisture must be retained within the samples [9].

4.2.2 Effect of NaOH Concentration

An increase in NaOH concentration led to an increase in compressive strength. The 2.5 M samples attained the lowest compressive strengths, while the 12.5 M samples achieved the highest compressive strengths. The percent increases in strength between samples of consecutive NaOH concentrations were not consistent.

In the exposed curing condition, the largest increase in strength after one day of curing occurred when the concentration was raised from 2.5 M to 5.0 M. This percent of increase ranged from 70% to 99%. As seen in Figures 17-19, after three days of curing, there was a large increase in strength between the 7.5 M and 10.0 M samples. This percent increase ranged from 91% to 130%. After seven days of curing, the large increase in compressive strengths between the 7.5 M and 10.0 M samples continued, spanning from 71% to 152%.

Figures 20-22 display the effect of NaOH concentration on the compressive strengths achieved by the samples in the moisture curing condition. The trends shown as the concentration

increased vary greatly from those trends identified for the exposed curing samples. At one day of curing, there is little difference in compressive strength between samples of variable concentration. Over the entire testing period, there is less than a 21% difference in compressive strengths between the 2.5 M and 5.0 M samples. At three days of curing, the compressive strengths began to differentiate themselves from one another, showing greater distinction between strength values achieved by each NaOH concentration. For the 0.50 s/b ratio samples, the largest percent increase occurred between the 5.0 M and 7.5 M samples. The 0.54 and 0.58 s/b ratio mixtures also showed large increases in compressive strength between molarities, but these increases occurred between the 7.5 M and 10.0 M samples and 10.0 M and 12.5 M samples respectively. These percent increases were 46% for the 0.54 s/b and 95% for the 0.58 s/b. After seven days of curing, the percent increases between these samples continued to widen.

The sealed curing condition exhibited trends similar to those found in the moisture curing condition. The results are shown in Figures 23-25. Initially when tested at one day, the samples showed little difference in strength due to concentration. Also similar to the moisture curing samples, the sealed curing samples began to show differences between compressive strengths due to concentration at three days. These differences continued to expand up to seven days. Unlike the moisture curing samples, the largest percent increase due to concentration was seen between the 2.5 M and 5.0 M samples. This increase ranged from 98% to 117% after seven days of curing.

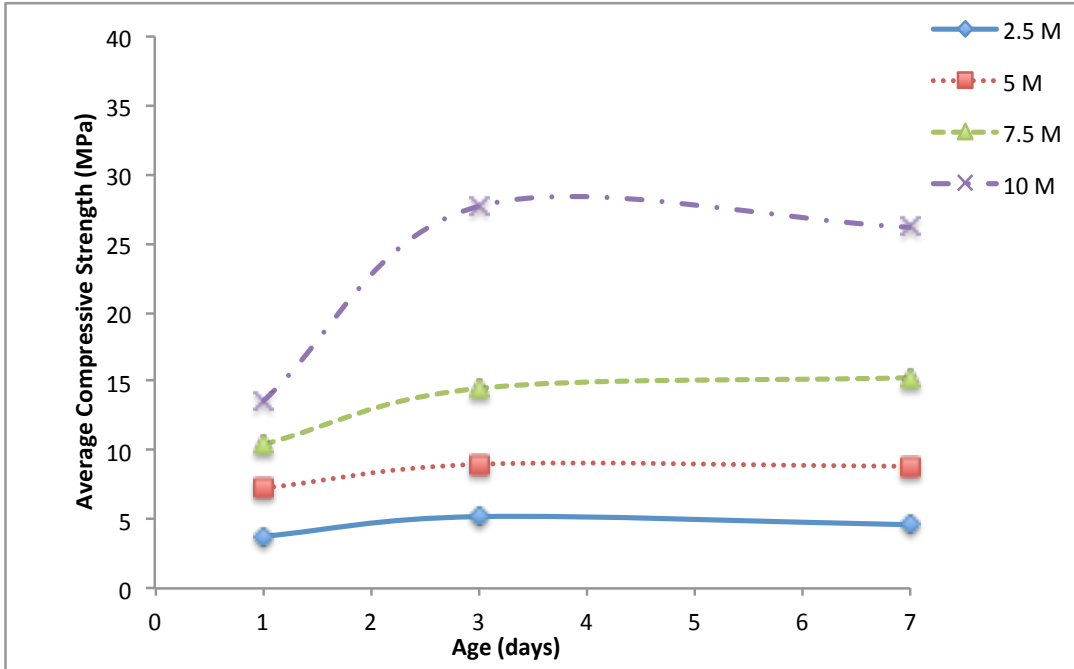


Figure 17: Effect of NaOH Concentration on Compressive Strength, 0.50 S/B Ratio Exposed Curing

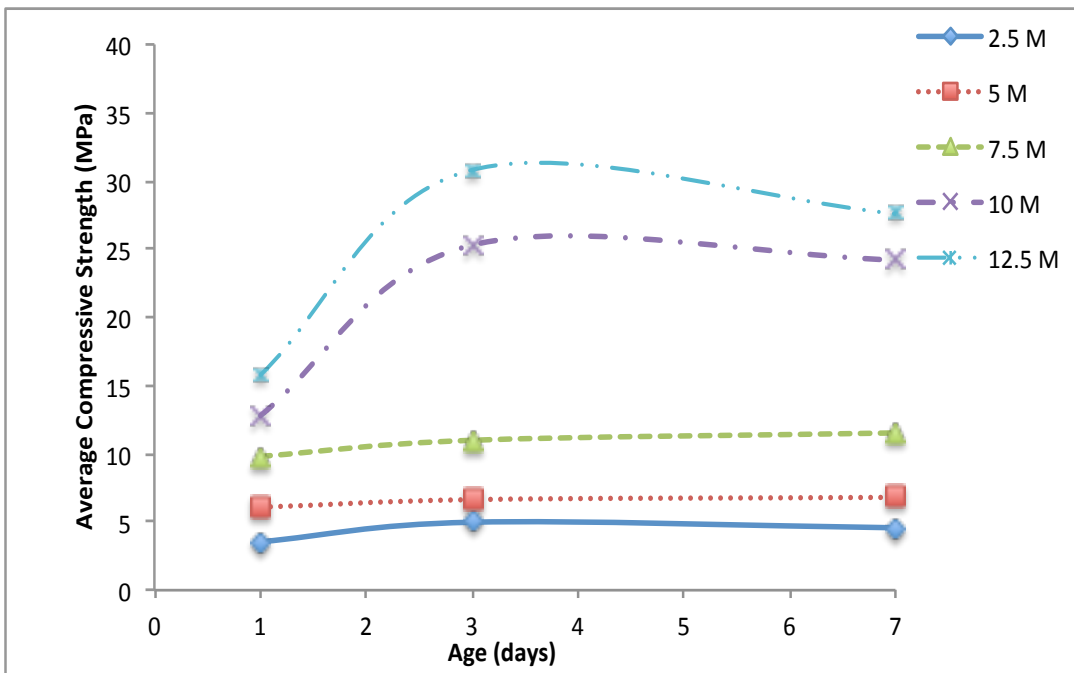


Figure 18: Effect of NaOH Concentration on Compressive Strength, 0.54 S/B Ratio Exposed Curing

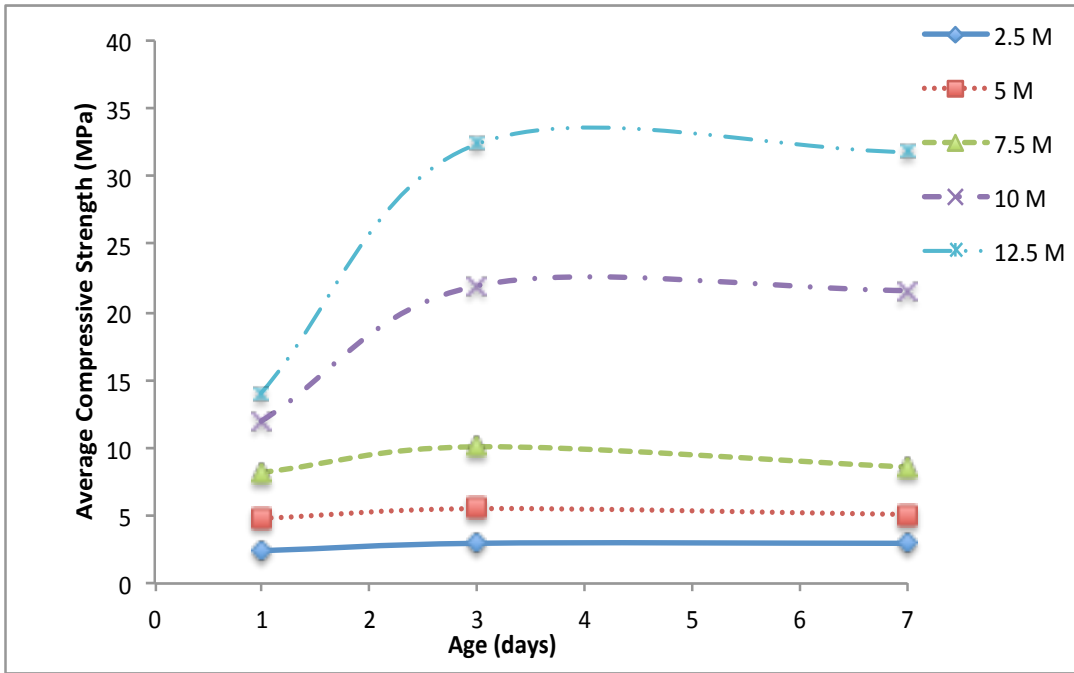


Figure 19: Effect of NaOH Concentration on Compressive Strength, 0.58 S/B Ratio Exposed Curing

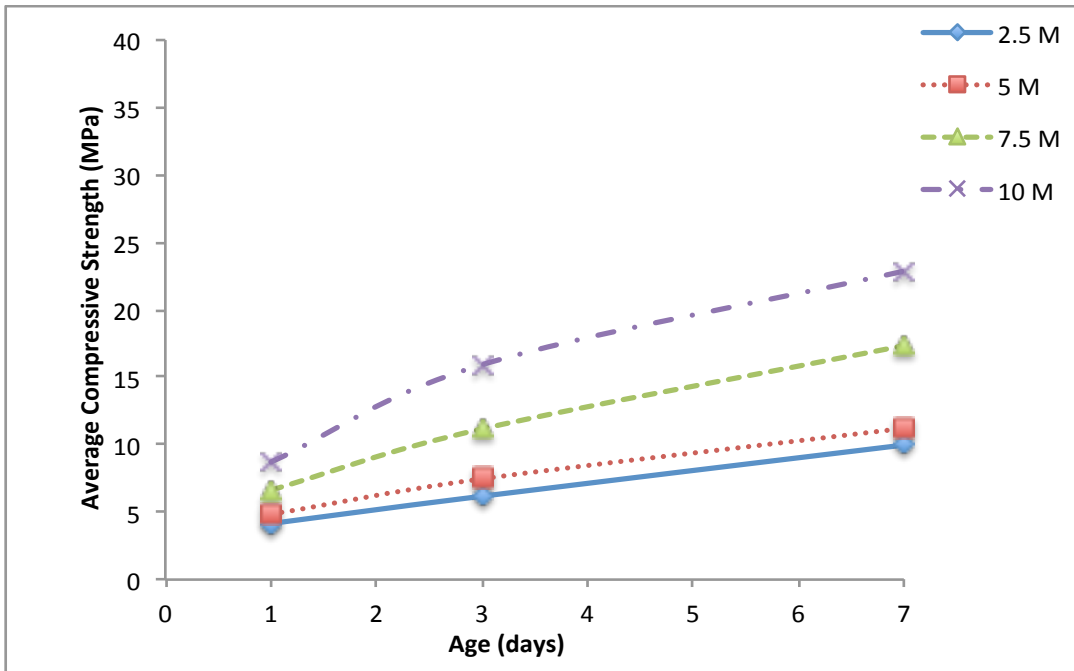


Figure 20: Effect of NaOH Concentration on Compressive Strength, 0.50 S/B Ratio Moisture Curing

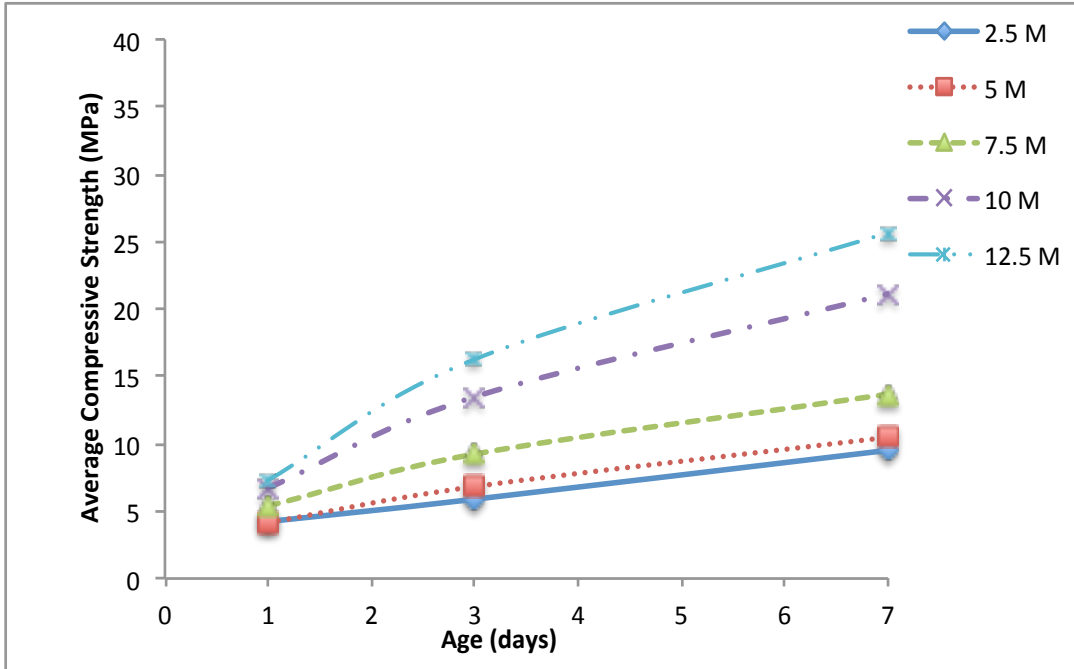


Figure 21: Effect of NaOH Concentration on Compressive Strength, 0.54 S/B Ratio Moisture Curing

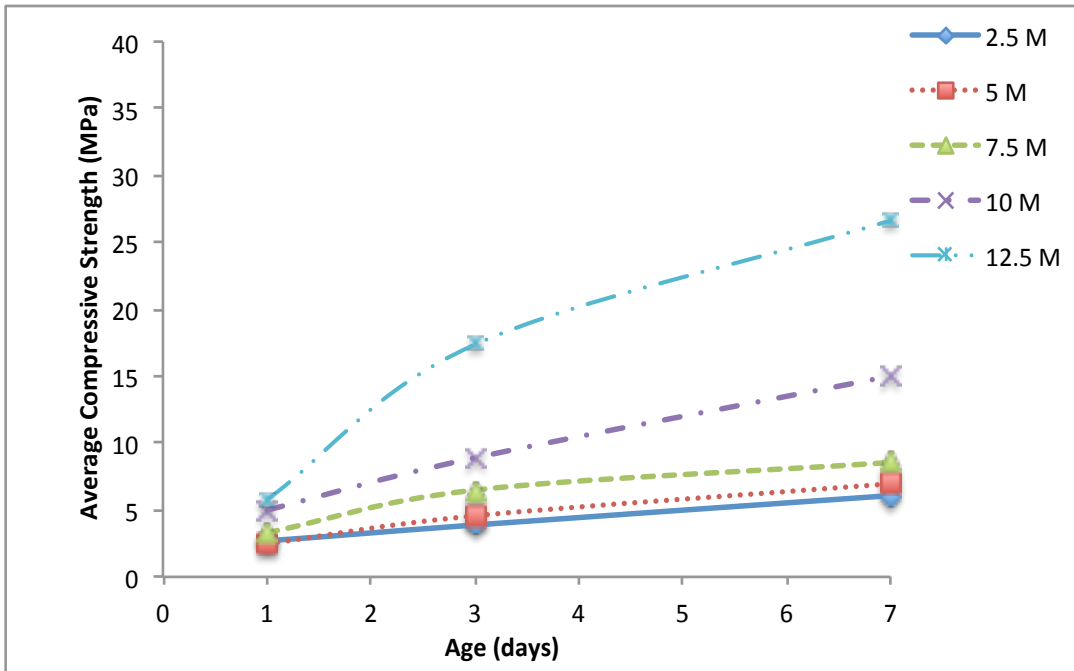


Figure 22: Effect of NaOH Concentration on Compressive Strength, 0.58 S/B Ratio Moisture Curing

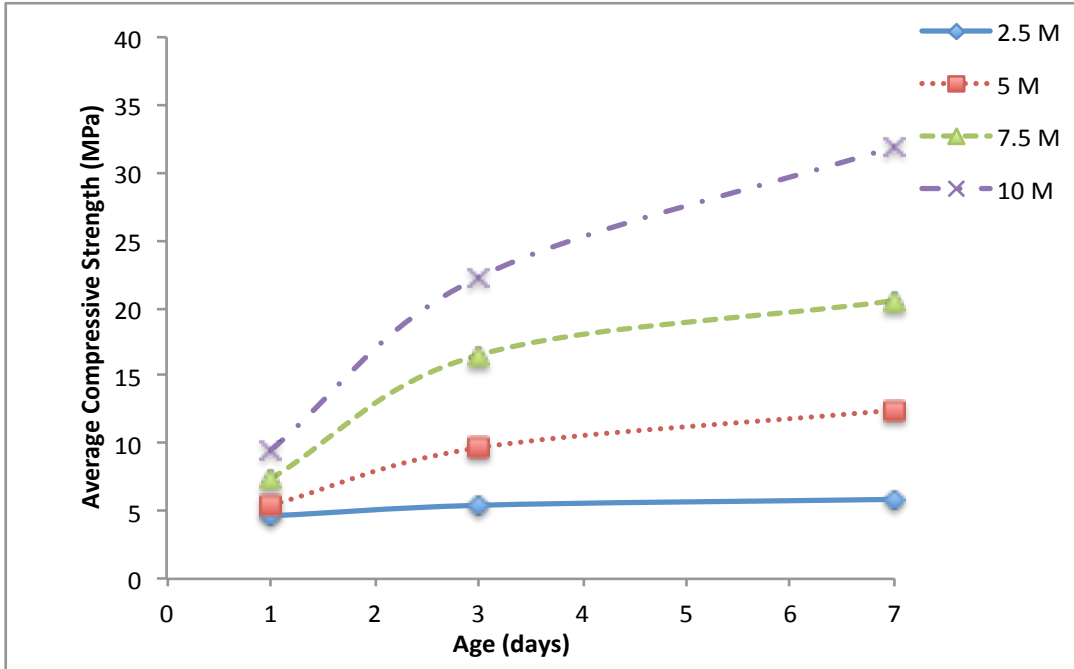


Figure 23: Effect of NaOH Concentration on Compressive Strength, 0.50 S/B Ratio Sealed Curing

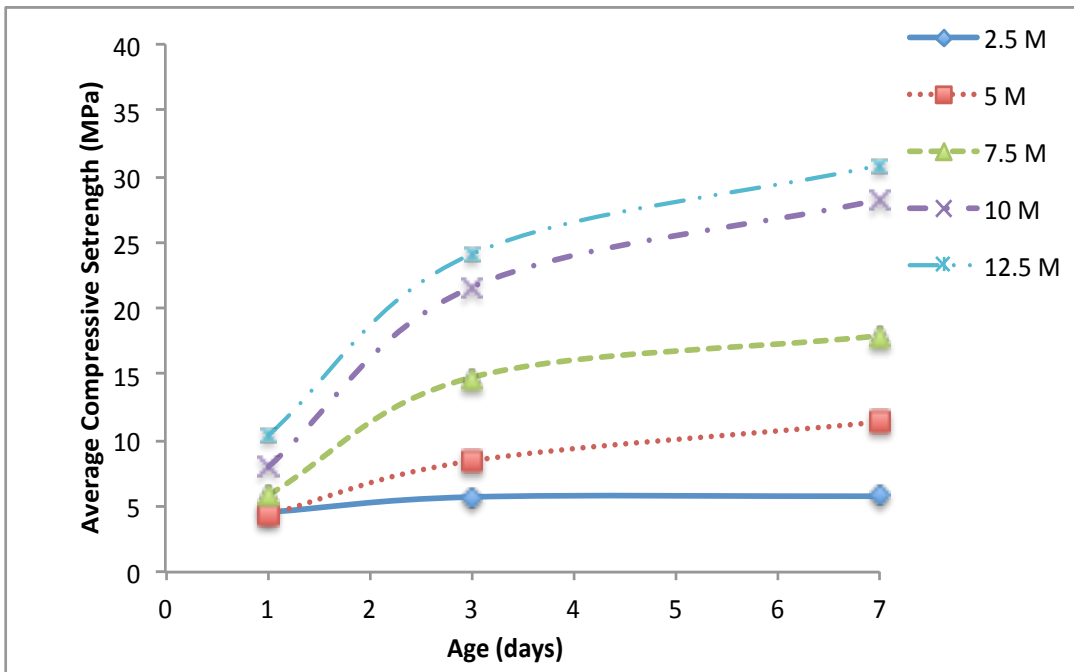


Figure 24: Effect of NaOH Concentration on Compressive Strength, 0.54 S/B Ratio Sealed Curing

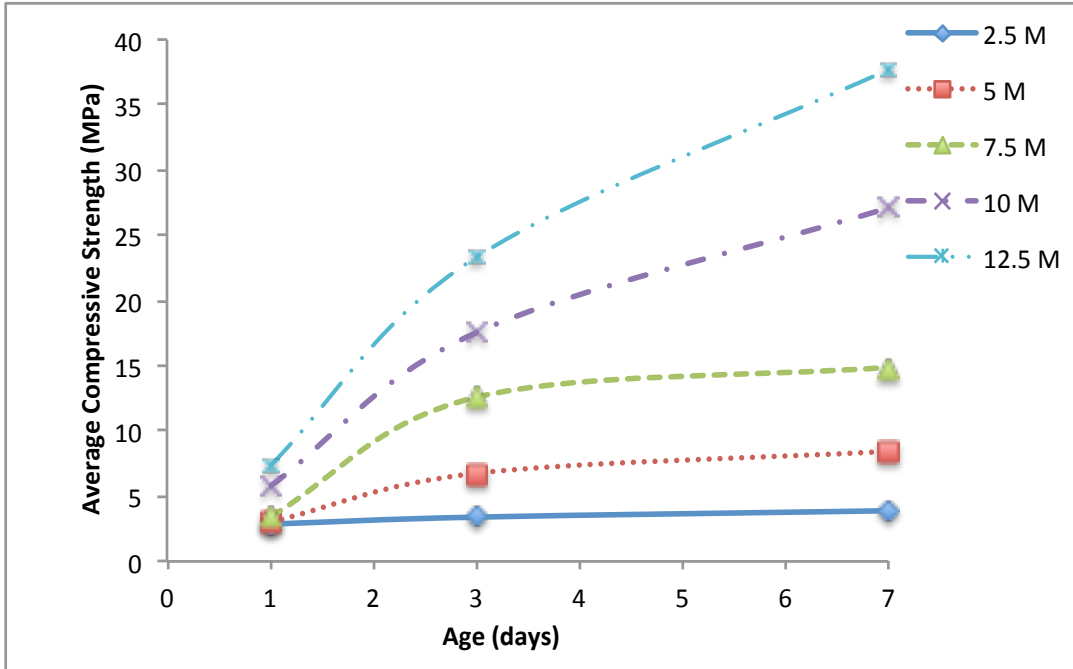


Figure 25: Effect of NaOH Concentration on Compressive Strength, 0.58 S/B Ratio Sealed Curing

As the NaOH concentration increased, the compressive strength also increased. This confirms that larger hydroxide concentrations are able to provide greater aluminosilicate solubility, leading to improved compressive strength [15]. This study also supported previous results showing that alkali activators with concentrations less than 5.0 M achieved little dissolution of the natural pozzolans, resulting in lower compressive strengths [15]. The exposed and sealed curing conditions showed large increases in compressive strength between the 2.5 M and 5.0 M samples, indicating that 2.5 M NaOH provided inadequate activation.

Amongst the various curing environments, large percent increases in compressive strength occurred between different concentrations. In the exposed curing condition, there was a large increase in strength between the 7.5 M and 10.0 M samples at three days of curing. This is indicative of the higher hydroxide concentration allowing for an increase in aluminosilicate solubility. After one day of curing, the differences in strength were not significant due to the 10.0 M samples' higher viscosity. However, once the samples were allowed to cure for a longer

time, the 10.0 M samples experienced adequate excess water evaporation, leading to greater bond formation and compressive strength.

The large increase in strength at three days between the 5.0 M and 7.5 M samples with the 0.50 s/b ratio in the moisture curing condition suggests that at this s/b ratio, the 7.5 M solution allowed for more activation to occur. This was noticed at three days due to the 7.5 M solution requiring a longer time for the excess water to evaporate. As the s/b ratio increased, the significant increases in strength occurred between different samples. The 0.54 s/b ratio samples saw a large increase in strength between 7.5 M and 10.0 M, while the 0.58 s/b ratio samples experienced a large increase in strength between 10.0 M and 12.5 M. This most likely occurred due to the reduction of natural pozzolans available for reaction. As the s/b ratio increased, there were fewer pozzolans included in the mixture, creating less opportunities for activation. Therefore, a higher concentration solution was required to increase the activation and bond formation. The 10.0 M solution was able to achieve more activation than the 7.5 M solution at the 0.54 s/b ratio, while the 12.5 M solution was required to significantly increase the activation of the 0.58 s/b ratio mixture.

The sealed curing samples showed growth trends similar to the moisture curing samples. Initially after one day of curing, there was little difference between the compressive strengths. In fact, as the concentrations increased, the percent of ultimate strength achieved after one day of curing tended to decrease. This supports the idea that high viscosity mixtures require more time for excess water evaporation and bond formation [15]. Additionally, from one to three days, the higher viscosity mixtures have had adequate time for bond formation, showing a larger increase in strength gain than samples made with lower viscosity solutions. Overall, the 10.0 M and 12.5 M samples in all curing conditions took longer to gain strength due to their increased viscosities.

4.2.3 Effect of Solution-to-Binder Ratio

The three s/b ratios tested were 0.50, 0.54, and 0.58. In general, the mixtures made with lower s/b ratios reached higher compressive strengths. The 12.5 M mixtures were the exception to this trend.

In the 2.5 M series of mixtures (Figure 26-28), there was little difference between the performances of the 0.50 and 0.54 s/b ratio mixtures. The largest increase due to reducing the s/b ratio from 0.54 to 0.50 was only 7%. In contrast, there was a sizable increase in compressive strength when the s/b ratio was reduced from 0.58 to 0.54. The percent increases in strength ranged from 48% to 68%.

The 5.0 M, 7.5 M, and 10.0 M samples exhibited a similar trend. The largest percent increases in strength due to s/b ratio resulted from the reduction of 0.58 to 0.54, comparable to what was shown in the 2.5 M series. The difference between the 2.5 M series and these mixtures is the percent increase in strength caused by reducing the s/b ratio from 0.54 to 0.50. For the 5.0 M, 7.5 M, and 10.0 M mixtures, there was a larger increase in strength than there was for the 2.5 M mixtures.

The 5.0 M and 7.5 M series showed increases in compressive strength resulting from reducing s/b ratios from 0.58 to 0.54 that ranged from 9% to 34% for the exposed curing condition and 42% to 68% for the moisture curing condition. Figures 29-31 show the trends for the 5.0 M series and Figures 32-34 display the results for the 7.5 M mixtures. The sealed curing condition displayed a wider range of compressive strength increases as a result of the same reduction in s/b ratio, ranging from 17% to 69%. The 69% increase in strength occurred for the reduction of s/b ratio from 0.58 to 0.54 for the 7.5 M samples after one day of curing. Mixtures

made from these concentrations (5.0 M and 7.5 M) showed anywhere from 7% to 36% increases in strength when going from s/b ratios of 0.54 to 0.50.

The 10.0 M series is shown in Figures 35-37. These samples increased by 8% to 15% in compressive strength when reducing the s/b ratio from 0.58 to 0.54 in the exposed curing condition. For comparison, the percent increase in strength was only 6% to 10% when going from s/b ratios of 0.54 to 0.50 in the exposed curing condition. The moisture curing samples showed larger increases in strength than the exposed curing samples. The range spanned from 34% to 52% larger strengths due to the reduction of s/b ratio from 0.58 to 0.54. The range when reducing the s/b ratio from 0.54 to 0.50 in moisture curing was 8% to 30%. The sealed curing samples also showed greater strength gain than the exposed curing samples when the s/b ratio was reduced from 0.58 to 0.54. This range spanned from 23% to 39% for one and three days of curing. At seven days, the largest strength gain was found when the s/b ratio was lowered to 0.50 from 0.54, achieving an improvement of 13%.

The 12.5 M samples showed a different trend than all of the other samples (Figures 38-40). After one day of curing, the 0.54 s/b ratio samples had higher compressive strengths than the 0.58 s/b ratios. The increases in compressive strengths ranged from 12% to 40% due to the reduction in s/b ratio from 0.58 to 0.54. At three days of curing, the trend began to switch. The sealed curing samples made with the 0.54 s/b ratio maintained higher compressive strengths than the 0.58 s/b ratio samples, however the moisture and sealed curing 0.58 s/b ratio samples exceeded the strengths achieved by the 0.54 s/b ratio samples. At seven days, all of the 0.58 s/b ratio samples were stronger than the 0.54 s/b ratio samples. These percent increases ranged from 4% to 22%.

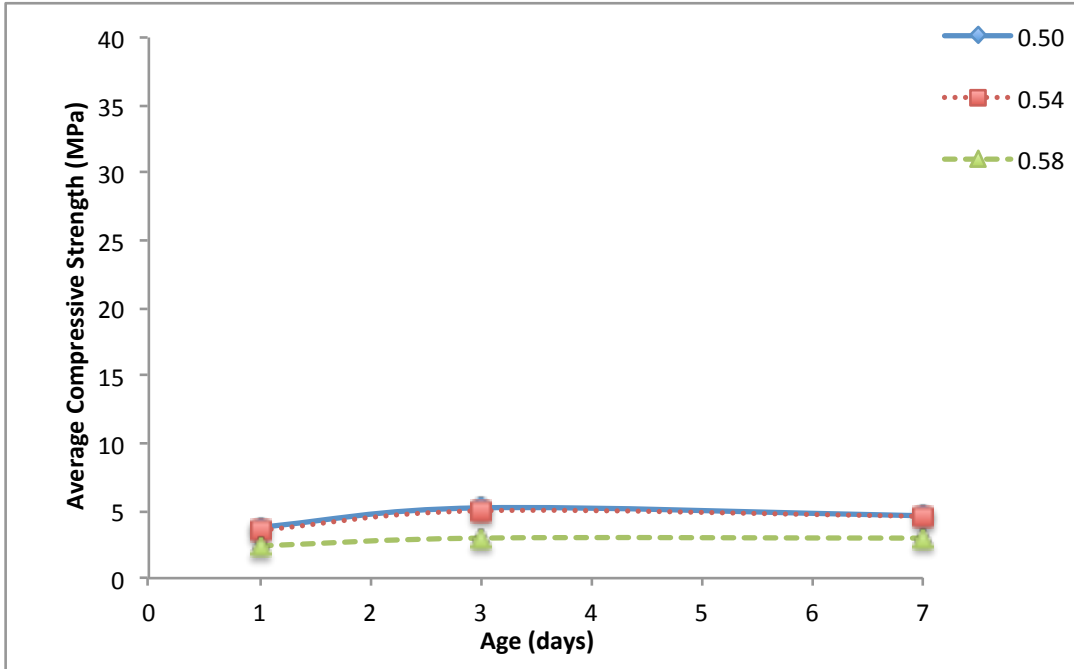


Figure 26: Effect of Solution-to-Binder Ratio on Compressive Strength, 2.5 M Exposed Curing

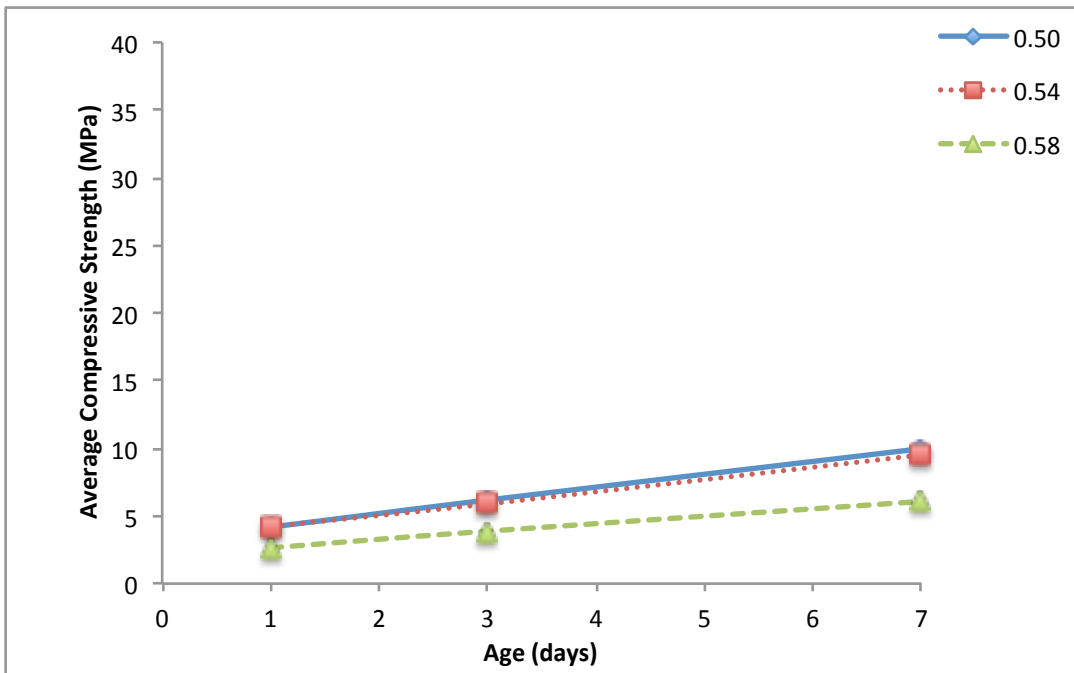


Figure 27: Effect of Solution-to-Binder Ratio on Compressive Strength, 2.5 M Moisture Curing

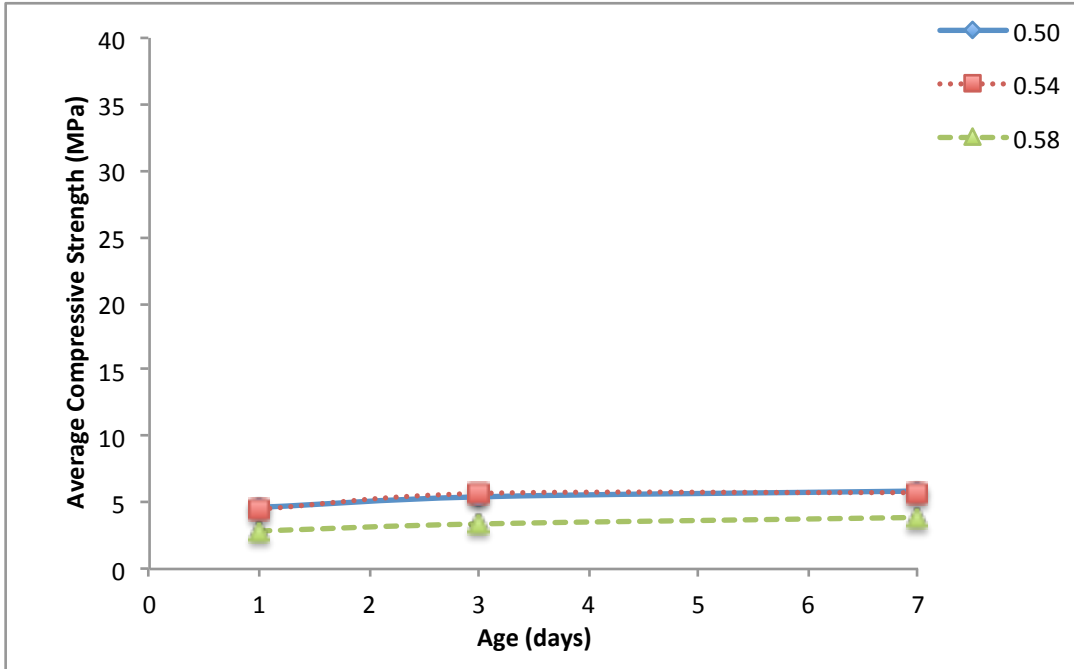


Figure 28: Effect of Solution-to-Binder Ratio on Compressive Strength, 2.5 M Sealed Curing

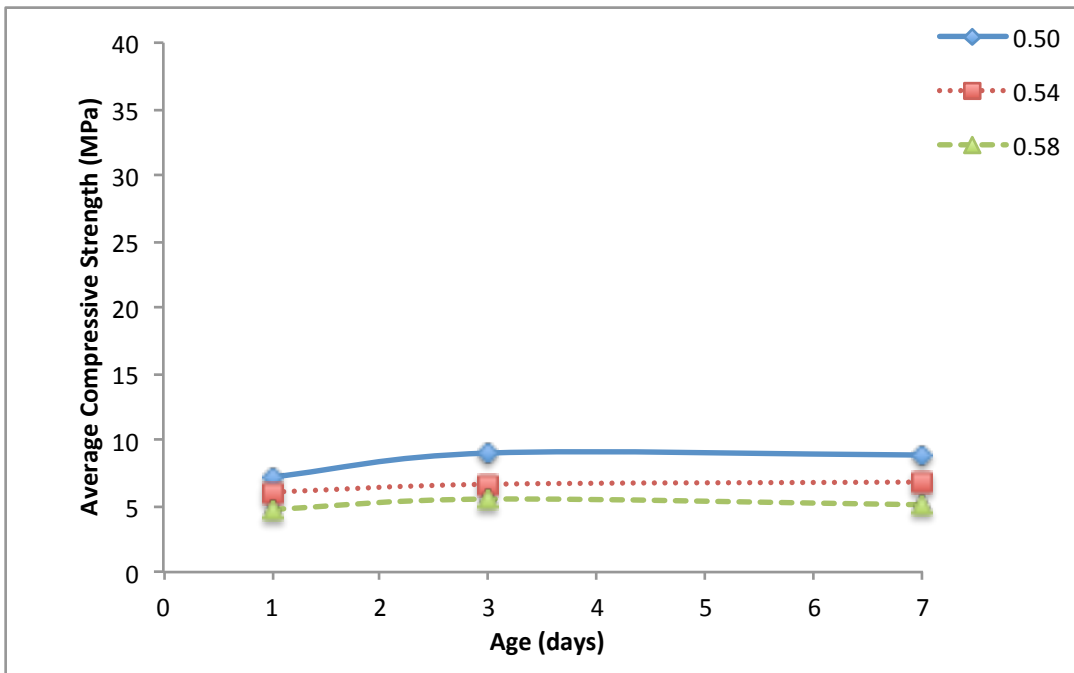


Figure 29: Effect of Solution-to-Binder Ratio on Compressive Strength, 5.0 M Exposed Curing

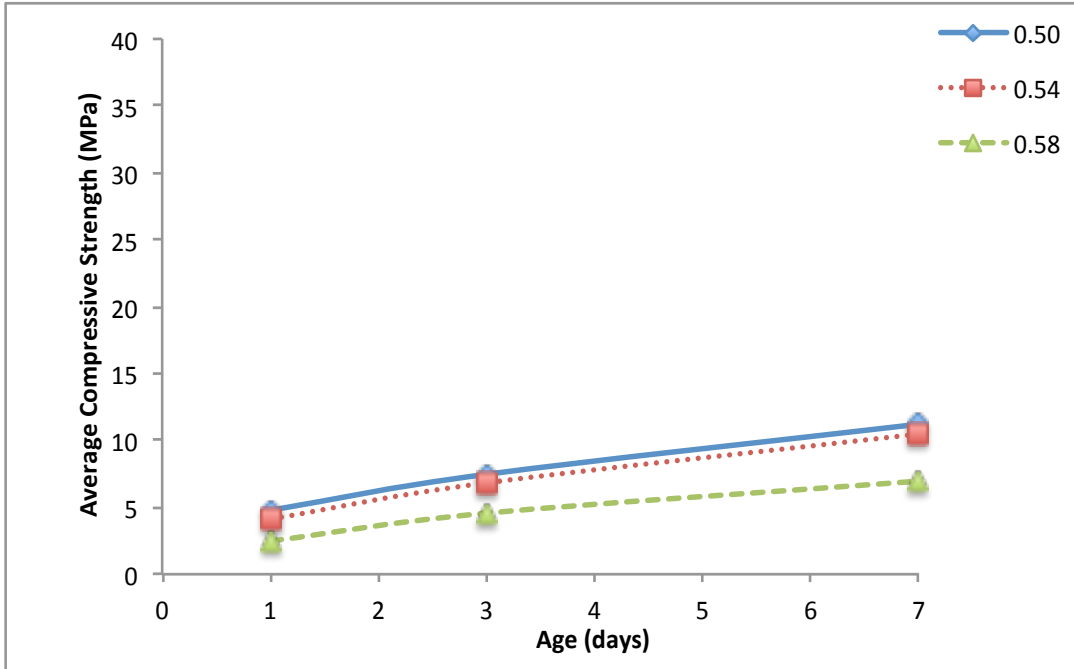


Figure 30: Effect of Solution-to-Binder Ratio on Compressive Strength, 5.0 M Moisture Curing

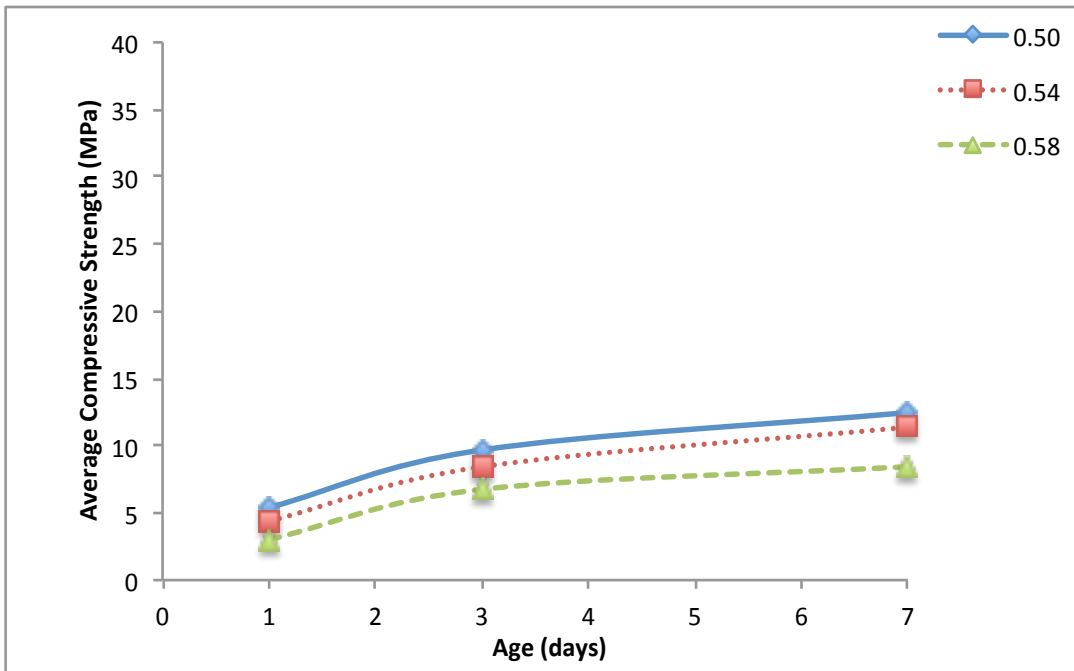


Figure 31: Effect of Solution-to-Binder Ratio on Compressive Strength, 5.0 M Sealed Curing

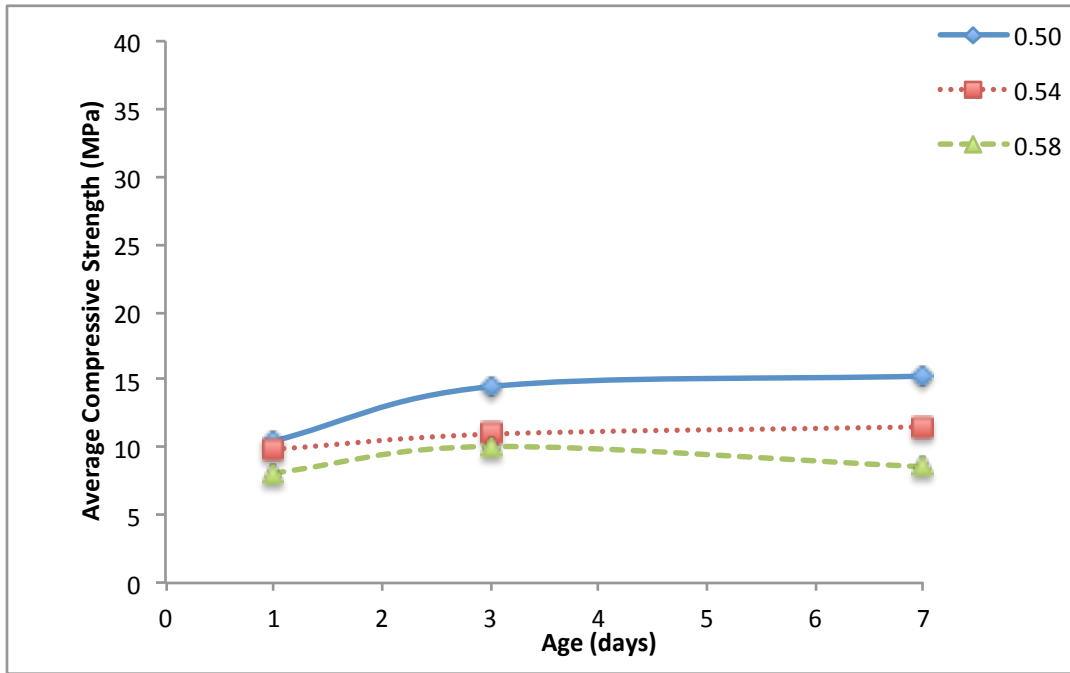


Figure 32: Effect of Solution-to-Binder Ratio on Compressive Strength, 7.5 M Exposed Curing

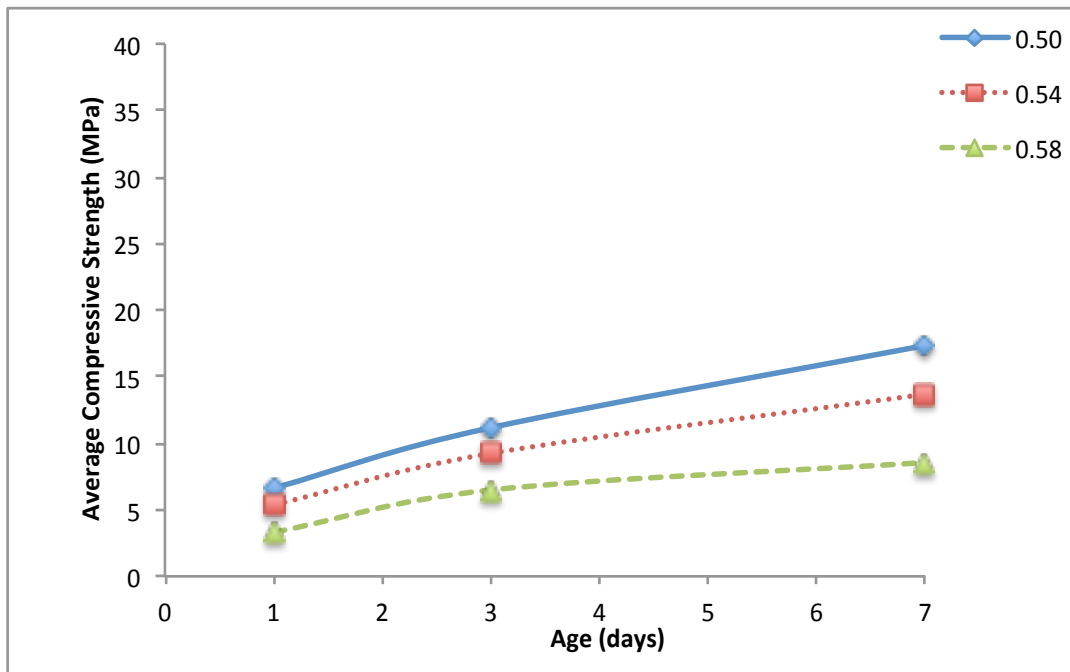


Figure 33: Effect of Solution-to-Binder Ratio on Compressive Strength, 7.5 M Moisture Curing

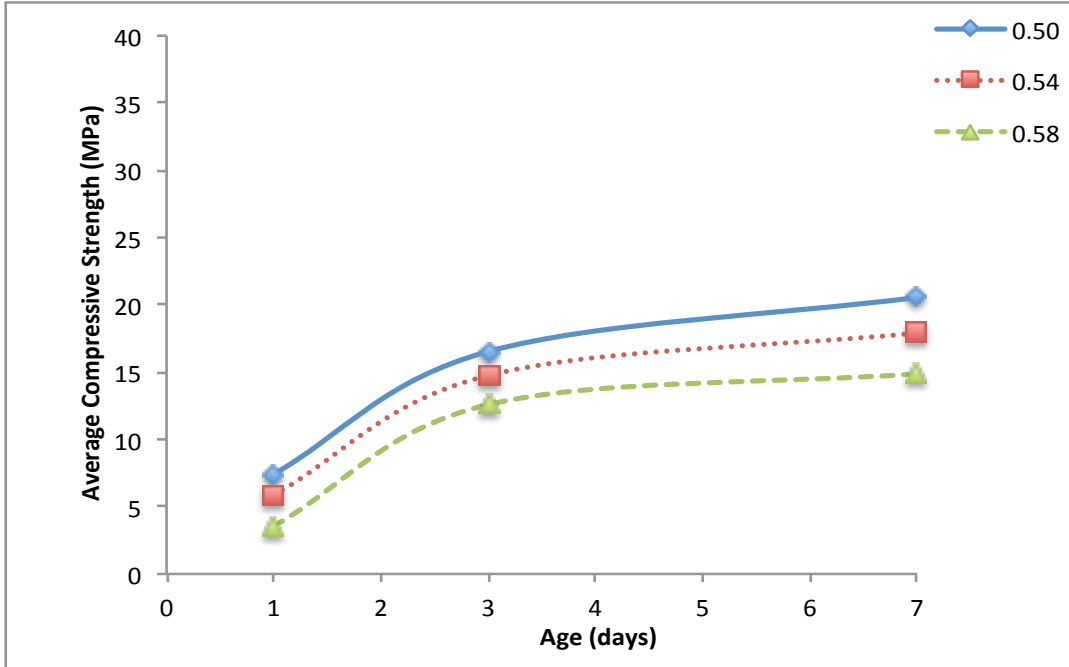


Figure 34: Effect of Solution-to-Binder Ratio on Compressive Strength, 7.5 M Sealed Curing

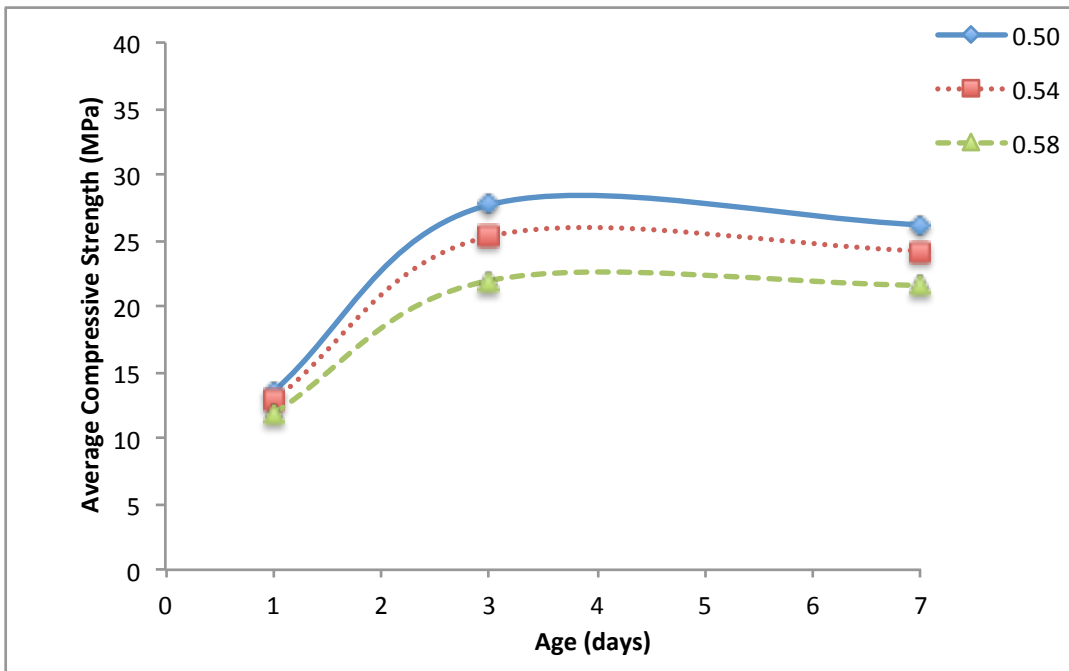


Figure 35: Effect of Solution-to-Binder Ratio on Compressive Strength, 10.0 M Exposed Curing

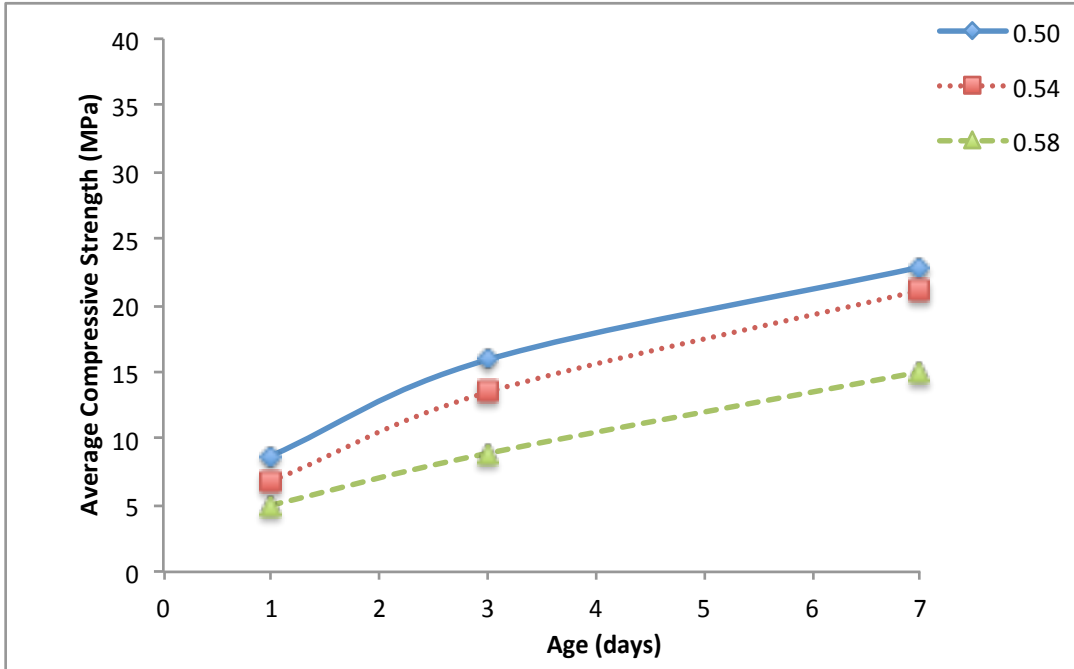


Figure 36: Effect of Solution-to-Binder Ratio on Compressive Strength, 10.0 M Moisture Curing

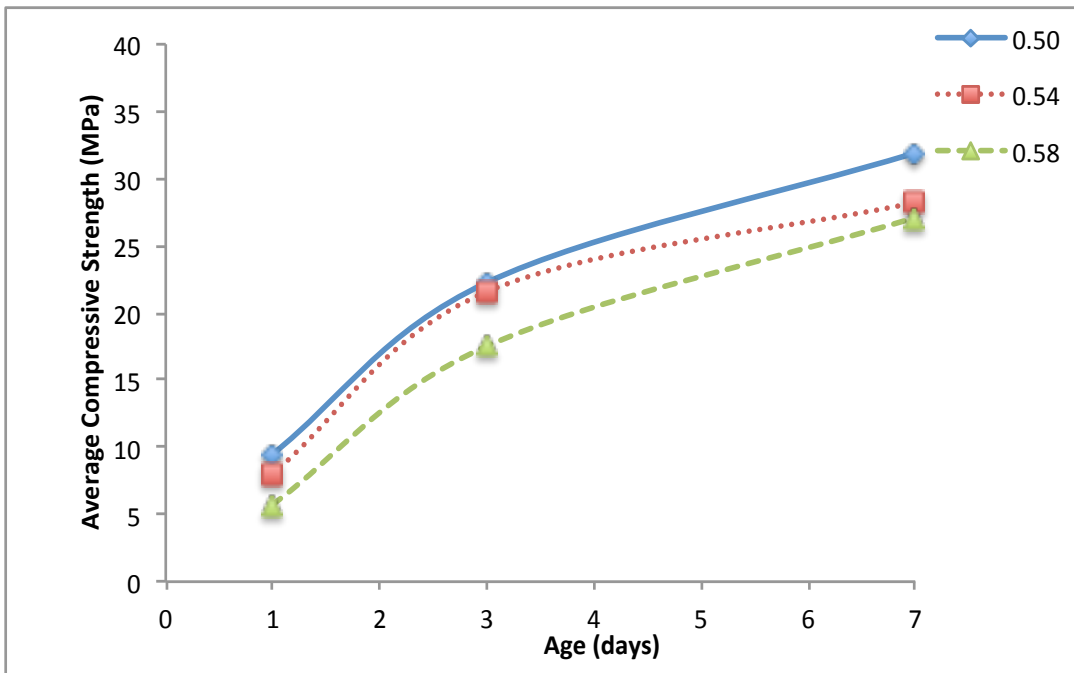


Figure 37: Effect of Solution-to-Binder Ratio on Compressive Strength, 10.0 M Sealed Curing

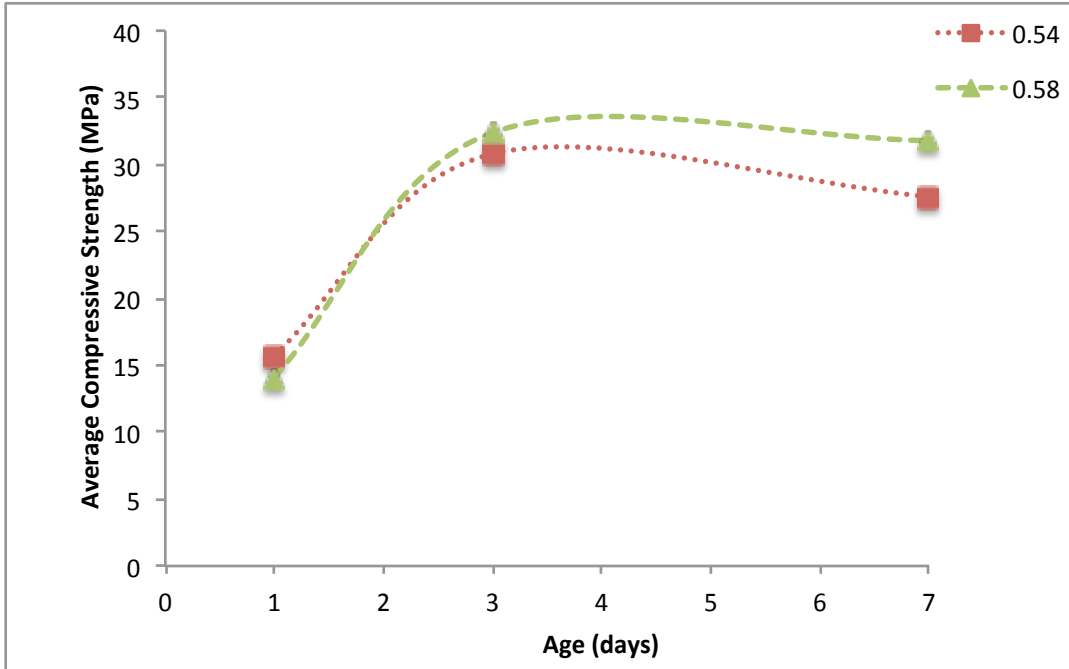


Figure 38: Effect of Solution-to-Binder Ratio on Compressive Strength, 12.5 M Exposed Curing

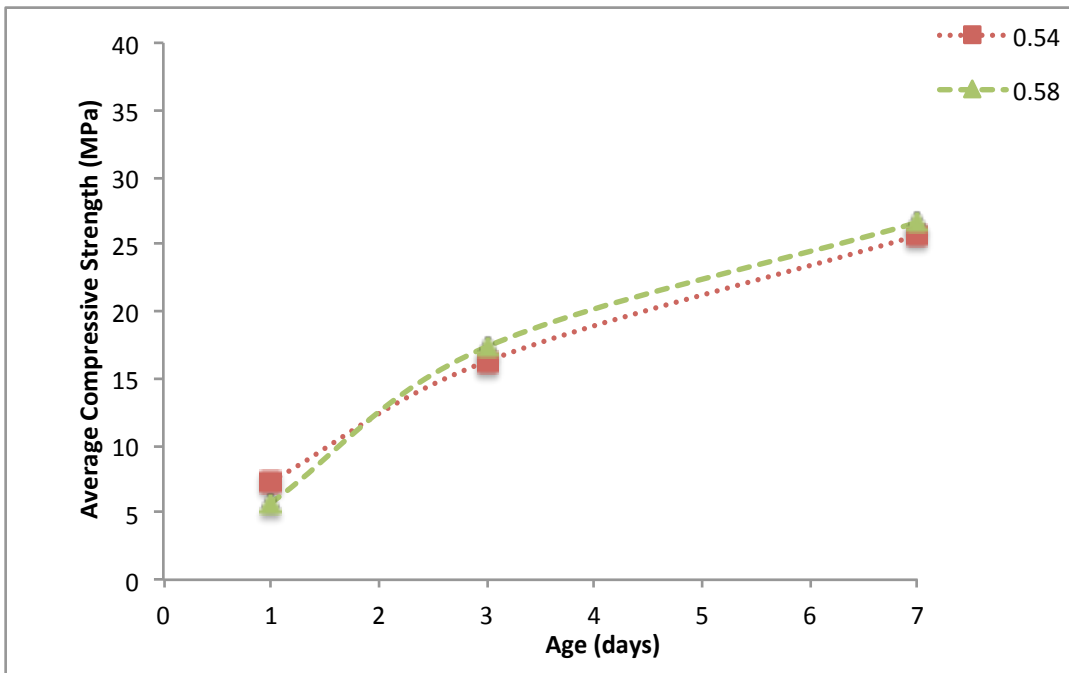


Figure 39: Effect of Solution-to-Binder Ratio on Compressive Strength, 12.5 M Moisture Curing

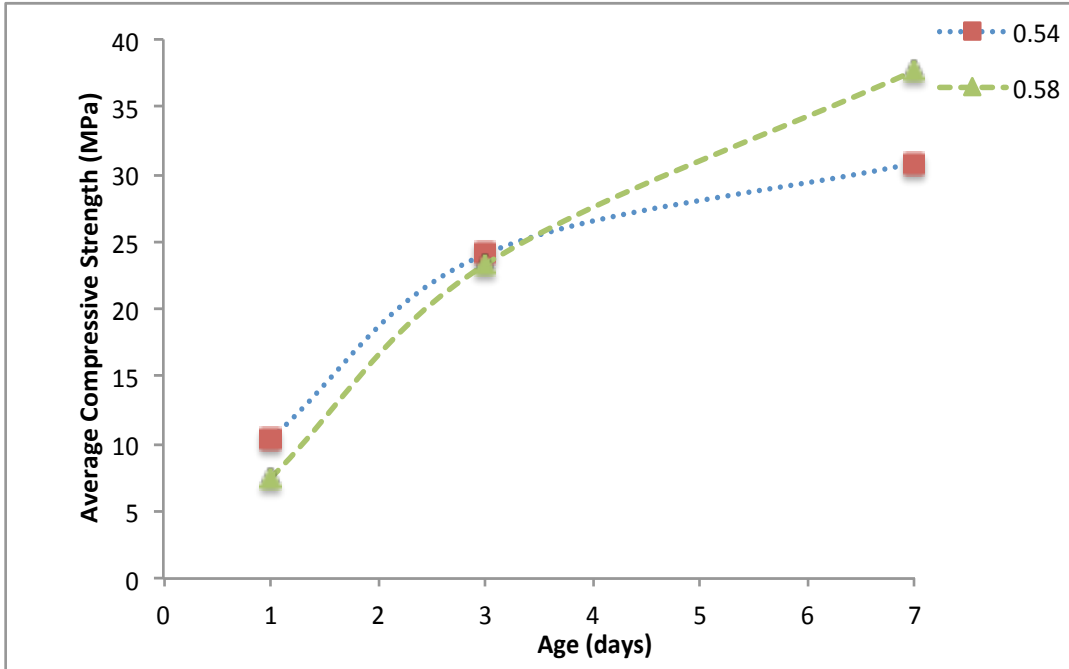


Figure 40: Effect of Solution-to-Binder Ratio on Compressive Strength, 12.5 M Sealed Curing

With the exception of the 12.5 M series, as the s/b ratio increased, the compressive strength decreased. This is similar to the trend produced by OPC. Previous work with geopolymers produced similar findings [9].

Reducing the s/b ratio from 0.58 to 0.54 produced the largest percent increase in strength. This is most likely due to the reduction of natural pozzolans present in the 0.58 s/b ratio mixtures, resulting in even fewer opportunities for bond formation. The difference between the 0.54 and 0.50 s/b ratios is less significant because both solutions contain larger amounts of natural pozzolans, so the quantity of solution added is not as important.

Furthermore, the exposed curing samples experienced less of an impact on compressive strength due to s/b ratio than the moisture and sealed curing samples. This can be explained by the dry conditions the exposed curing samples are cured in. Excess water was able to evaporate more easily, causing the s/b ratio to have less of an impact. The 2.5 M, 5.0 M, and 7.5 M samples showed larger increases in strength as the s/b ratios are reduced than the 10.0 M and

12.5 M samples. This shows that with the higher concentration NaOH samples, the s/b ratio is a secondary factor with regards to compressive strength.

The 12.5 M samples exhibited a unique trend from the other samples. After one day of curing, the 0.54 s/b ratio samples performed better than the 0.58 s/b ratio samples due to the addition of less water to the mixture. Therefore, evaporation of excess water was able to occur more quickly, contributing to the higher compressive strength. At three days, the 0.58 s/b ratio samples performed better for the exposed and moisture curing conditions. The 0.54 s/b ratio sealed curing samples only performed 3% better than the 0.58 s/b ratio samples, so these samples were also nearing the transition phase at three days where the 0.58 s/b ratio samples achieved more strength. At seven days, all of the 0.58 s/b ratio samples reached higher compressive strengths. This may be due to the reduced workability of the 0.54 s/b ratio mixtures when creating the samples.

4.2.4 Curing Room Samples

The samples cured in the curing room for 7 and 28 days did not show any significant strength gain. There is no common trend amongst the samples other than an increase in strength from 7 to 28 days as well as an increase in compressive strength with reduced s/b ratio. The only sample that differed from these trends was the 2.5 M 0.54 s/b ratio mixture. This mixture actually achieved higher compressive strengths than the 0.50 s/b ratio samples.

Overall, the largest 7-day compressive strength was attained by the 10.0 M 0.50 s/b ratio samples and the lowest compressive strength was achieved by the 7.5 M 0.54 s/b ratio samples. These values were 3.815 and 2.893 MPa, respectively. Additionally, the 10 M 0.50 s/b ratio samples achieved the largest 28-day compressive strength with 5.582 MPa and the lowest

strength was reached by the 12.5 M 0.58 samples with 2.406 MPa. These results are much different than those achieved by the oven curing samples. The results are reported in Table 4.

Table 4: Curing Room Average Compressive Strengths

NaOH Concentration	S/B Ratio	7-Day (MPa)	28-Day (MPa)
2.5 M	0.50	2.815	3.850
	0.54	3.365	5.105
	0.58	1.977	2.873
5.0 M	0.50	3.225	5.283
	0.54	2.194	3.649
	0.58	1.596	3.021
7.5 M	0.50	3.214	5.568
	0.54	2.893	4.785
	0.58	1.484	3.027
10.0 M	0.50	3.815	5.582
	0.54	2.740	4.421
	0.58	1.618	3.571
12.5 M	0.54	2.465	3.394
	0.58	1.587	2.406

The samples in the curing room showed little strength gain after 28 days of curing. This confirms that an oven curing environment ranging in temperature from 30°C to 90°C is most conducive to strength development [9]. Furthermore, higher temperature is needed to allow the formation for the monolithic geopolymer layer as was found by Bondar et al. [15]. This helps form a strong network of hydrates, improving the mortar’s overall performance. Since the curing room does not allow for evaporation of the excess water, little monolithic geopolymer is formed producing samples with low compressive strengths.

As the NaOH concentration was increased, there was not always an increase in compressive strength as was the case for the oven curing samples. In fact, the 12.5 M series of mixtures achieved the lowest 28-day compressive strengths. These results show the negative effect the curing room has on the strength development process for alkali-activated natural

pozzolans. In this environment, the additional activation provided by the higher concentration solutions does not improve the overall performance of samples.

Due to the low compressive strengths achieved by the samples in the curing room, no further testing was completed on these samples. There would be little practical application of these materials in the construction industry as they provide inadequate structural strength.

4.3 Flexural Strength

The ultimate strains, modulus of rupture, and 40% modulus of elasticity (stiffness) values are shown in Table 5. Overall, the modulus of rupture values increased with increasing NaOH concentration. Additionally, these values decreased with increasing s/b ratio. This trend was similar to that shown by the compressive strength results. The amount of strain varied amongst the samples, with no trend relative to NaOH concentration or s/b ratio.

Table 5: Flexure Properties

NaOH Concentration	S/B Ratio	Strain ($\mu\epsilon$)	Modulus of Rupture (MPa)	40% Modulus of Elasticity (MPa)
2.5	0.50	533	1.329	4330
	0.54	353	1.135	3616
	0.58	200	0.732	3481
5.0	0.50	270	2.766	13431
	0.54	795	2.783	9307
	0.58	335	2.524	8750
7.5	0.50	392	6.174	18155
	0.54	507	5.740	14694
	0.58	594	5.476	14018
10.0	0.50	385	7.074	19146
	0.54	458	6.562	17251
	0.58	431	6.665	16789
12.5	0.54	386	8.490	21554
	0.58	273	6.040	21137

The modulus of elasticity, or stiffness values, were reported at the 40% values of strain and modulus of rupture. This 40% value was selected as the cutoff point as it provided a clear representation of the impact NaOH concentration had on the stress-strain relationship of the mortars.

As the concentration increased, so too did the stiffness. The largest stiffness was exhibited by the 12.5 M sample with 0.54 s/b ratio and the smallest stiffness was shown by the 2.5 M 0.58 s/b ratio sample. The largest increase in stiffness was achieved when increasing the NaOH concentration from 2.5 M to 5.0 M. This change in molarity increased the stiffness by 151% to 210% for all of the s/b ratios. The subsequent increases in concentration up to 10.0 M exhibited smaller percent increases in stiffness between samples. The adjustment of concentration from 5.0 M to 7.5 M saw percent increases of 35% to 62%. When going from 7.5 M to 10.0 M, the percent increases reduced to 6% to 20%. When the concentrations were increased from 10.0 M to 12.5 M, the percent increases in stiffness were approximately 25%.

It should be noted that the lower NaOH concentration samples did not break quickly when the samples were loaded in the compressive machine. As the crack formed, the low concentration sample continued to bend without breaking fully apart. In contrast, the high concentration samples, such as those made with 10.0 M and 12.5 M NaOH, broke quickly and rigidly with little bending. This trend in breaking showed that the lower concentration solutions produced concrete with more flexibility whereas the higher concentrations produced samples that were more brittle in nature.

Lower s/b ratios corresponded with larger stiffness values. For all molarities, the lowest s/b ratio achieved the highest stiffness, while the 0.58 s/b ratios achieved the lowest stiffness values. The increase in stiffness when reducing the s/b ratio from 0.58 to 0.54 was negligible,

ranging from 2% to 7%. There was a larger increase as a result of reducing the s/b ratio from 0.54 to 0.50. These percent increases ranged from 11% to 44%. In general, the 2.5 M, 5.0 M, and 7.5 M samples showed larger percent increases in stiffness as a result of reducing the s/b ratio. The largest percent increase resulting from the reduction in s/b ratio occurred for the 5.0 M samples when decreasing the ratio from 0.54 to 0.50.

The flexural strength experienced by the samples followed a trend similar to the sealed curing samples. The largest stiffness was achieved by the 0.54 s/b ratio 12.5 M samples, which also attained the largest compressive strengths. Similarly, the lowest stiffness value was obtained by the 0.58 s/b ratio 2.5 M samples. This shows that compressive strength is an indicator of flexural strength.

As the NaOH concentration increased, more bonds were formed, producing samples with less flexibility. Samples with lower s/b ratios also exhibited greater bond formation and less flexibility. This resulted in the high concentration and low s/b ratio samples experiencing well-defined, rigid breaks.

The 2.5 M, 5.0 M, and 7.5 M samples also showed greater differences in stiffness due to s/b ratios. This is similar to the trend experienced by the samples for compressive strength results. In contrast to the compressive strength results, the largest percent increase in stiffness occurred when the s/b ratio was reduced from 0.54 to 0.50 instead of from 0.58 to 0.54.

Although the reduction in s/b ratio from 0.58 to 0.54 resulted in a greater increase in compressive strength, the reduction in s/b ratio from 0.54 to 0.50 had a larger impact on the strain experienced by each sample. Thus, the reduction in s/b ratio from 0.54 to 0.50 resulted in a larger increase in stiffness.

4.4 Density/Absorption/Voids

After seven days of sealed curing, the samples were examined for density, absorption, and void content. The results are summarized in Table 6 below.

Table 6: Average Density, Absorption, and Void Results

NaOH Concentration	S/B Ratio	Abs. after immers. (%)	Abs. after immers and boiling (%)	Bulk density, dry	Bulk density after immers.	Bulk density after immers. and boiling	App. Density	Volume of Perm. Pore space, voids
2.5 M	0.50	12.40%	13.62%	1.898	2.133	2.156	2.559	25.84%
	0.54	13.41%	15.28%	1.877	2.129	2.164	2.632	28.68%
	0.58	13.82%	15.66%	1.840	2.095	2.129	2.586	28.83%
5 M	0.50	10.33%	11.82%	1.943	2.144	2.172	2.522	22.95%
	0.54	11.26%	12.88%	1.903	2.094	2.124	2.484	24.25%
	0.58	11.52%	13.17%	1.907	2.130	2.161	2.552	25.16%
7.5 M	0.50	7.70%	8.42%	2.074	2.234	2.249	2.513	17.47%
	0.54	8.42%	9.38%	1.962	2.106	2.125	2.389	18.22%
	0.58	9.92%	12.17%	1.961	2.168	2.213	2.550	24.01%
10 M	0.50	3.94%	4.66%	2.100	2.180	2.195	2.332	9.54%
	0.54	5.47%	7.33%	2.038	2.149	2.187	2.374	14.94%
	0.58	6.41%	9.14%	1.961	2.087	2.140	2.390	17.93%
12.5 M	0.54	2.38%	4.36%	2.071	2.120	2.161	2.278	9.01%
	0.58	2.41%	5.70%	2.069	2.119	2.187	2.345	11.78%

The sample with the lowest dry bulk density (1.840) was the 2.5 M 0.58 s/b ratio mixture and the sample with the highest dry bulk density (2.100) was the 10.0 M 0.50 s/b ratio mixture. The dry bulk density was shown to decrease with increasing s/b ratio, however there was a diverse range of variation between samples. The NaOH concentration also affected the dry bulk density, indicating that increasing the concentration also increased the bulk density. The bulk density after immersion increased from the dry bulk density. Similarly, the bulk density after immersion and boiling further increased in value. These increases in bulk density were inconsistent, with no observable trend. In regards to the apparent density, the highest NaOH concentrations were shown to have smaller values than the lower NaOH concentrations.

The absorption of the samples after immersion and boiling were also investigated. The 2.5 M series of mixtures had the greatest absorptions after immersion ranging from 12.4% to 13.8%, while the 12.5 M series of mixtures had the lowest absorption after immersion values, around 2.4%. The mortar mixtures in between showed decreasing absorption after immersion values with increasing concentration. Absorption values for all of the concentrations increased after the samples were boiled. The 2.5 M series attained absorption values ranging from 13.6% to 15.7% while the 12.5 M series reached values of 4.4% to 5.7%. The absorption values also increased with increasing s/b ratios. It should be noted that the 0.58 s/b ratio series of mixtures experienced the most significant increases in absorption values after boiling compared to the values solely after immersion. These increases ranged from 1.7% to 3.3%. In comparison, the 0.54 s/b ratio series showed increases of 1.0% to 2.0% and the 0.50 s/b ratio series displayed increases of 0.7% to 1.5%.

The volume of void content showed a comparable trend to the absorption values. As the s/b ratio increased, the percentage of voids also increased. Additionally, the void content was reduced as the NaOH concentration increased. The sample with the largest void content (28.8%) was the 2.5 M 0.58 s/b ratio mixture while the sample with the lowest void content (9.0%) was the 12.5 M 0.54 s/b ratio mixture. Figures 41 and 42 display the trends present in the void content of the samples.

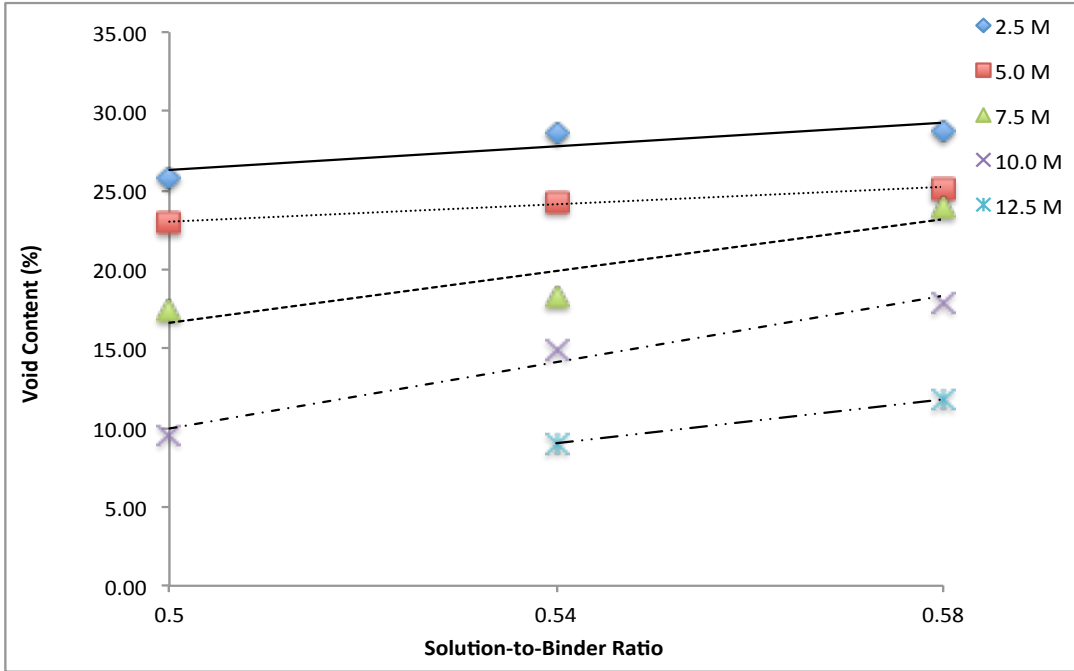


Figure 41: Effect of NaOH Concentration on 7-Day Void Content

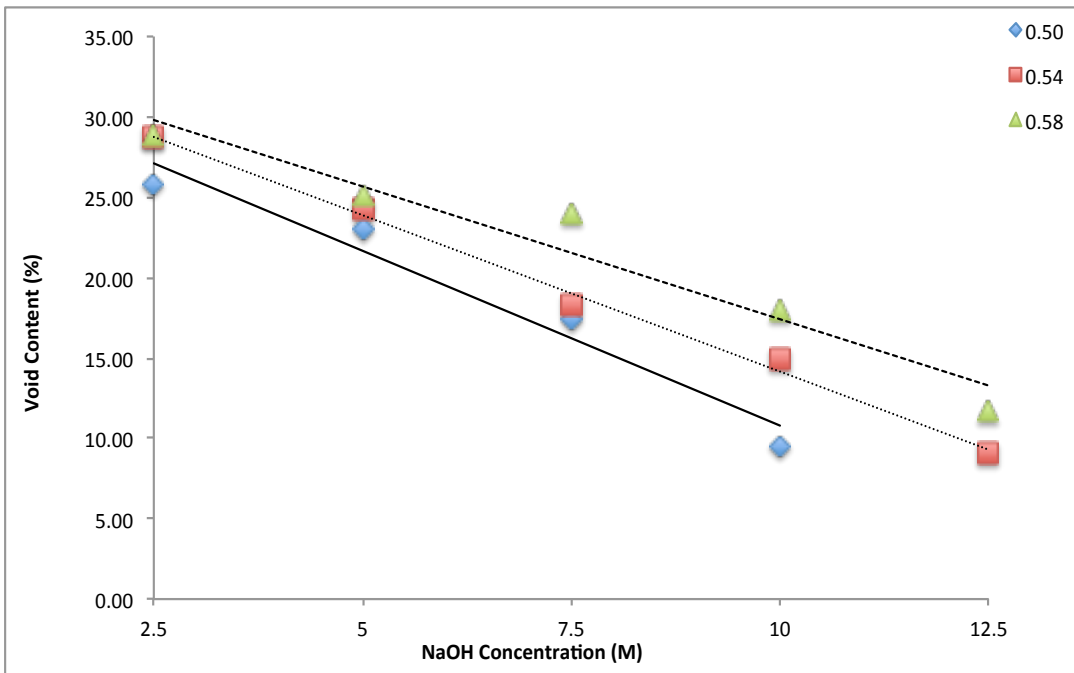


Figure 42: Effect of Solution-to-Binder Ratio on 7-Day Void Content

The bulk densities of the samples increased with increasing NaOH concentration. This supports the results obtained for the compressive strengths of the samples. Larger hydroxide concentrations produced greater alkali activation, leading to more bond formation and strength gain [15]. With more bonds forming within the mortar, there is less room for voids within the samples. This correlates directly with the results achieved for absorption. The most absorption occurred within the 2.5 M series of samples, while the least absorption occurred within the 12.5 M samples.

Raising the s/b ratio also increased the amount of absorption experienced by the samples. With larger s/b ratios, there was a reduction in compressive strength as seen in this study. Smaller compressive strengths indicate that there have been fewer bonds forming within the mortar. This leads to more void content within the samples. Overall, samples cured in elevated temperature conditions show that compressive strength has an inverse relationship with absorption and void content. Samples with larger compressive strengths typically have smaller absorption and void content. There is a direct relationship between compressive strength and density. With greater bond formation, there is less empty space contained within the given volume of a sample, leading to higher densities.

4.5 Rapid Chloride Penetration Test

The sealed curing samples tested at seven days showed the following results summarized in Table 7.

Table 7: Average RCPT Results

NaOH Concentration	S/B Ratio	7-Day Adjusted Charge Passed (Coulombs)	Initial Current at 10 V (mA)
2.5 M	0.50	6118	270.3
	0.54	6308	299.1
	0.58	6800	356.8
5.0 M	0.50	6625	374.6
	0.54	---	---
	0.58	6776	481.8
7.5 M	0.50	6239	334.5
	0.54	6433	331.2
	0.58	7080	439.0
10.0 M	0.50	2407	124.4
	0.54	3463	182.4
	0.58	6397	311.7
12.5 M	0.54	1054	55.5
	0.58	1064	62.3

--- refers to samples that exceeded the testing equipment's capacity

With increasing s/b ratio, the amount of charge passed also increased. The amount of increase varied with the concentration. The 10.0 M concentration mixture showed the largest increase in charge passed resulting from increasing the s/b ratio. As the s/b ratio was raised from 0.50 to 0.54, the amount of charge passed increased by 43.9%. The increase was even larger when the s/b ratio was raised from 0.54 to 0.58, increasing the charge passed by 84.7%.

In the 0.50 s/b ratio series of mixtures, the 5.0 M samples passed the highest number of coulombs. The 7.5 M reported the highest charge passed for the 0.54 s/b series of mixtures, however it should be noted that the 5.0 M samples overflowed the testing apparatus at this s/b ratio so no data was obtained. In the 0.58 s/b ratio mixtures, the 7.5 M samples passed the most charge. Overall, the 7.5 M 0.58 s/b ratio samples passed the greatest amount of charge with

7,080 coulombs. The least amount of charge was passed by the 12.5 M 0.54 s/b ratio samples with 1,054 coulombs.

The initial current flowing through the samples was also reported. Overall, the largest current was experienced by the 5.0 M NaOH concentration mixtures followed by the 7.5 M, 2.5 M, 10.0 M, and 12.5 M concentrations. Within the 0.50 s/b ratio samples, the 5.0 M mixture attained the highest initial current of 374.6 mA. The 0.54 s/b ratio series of mixtures displayed the highest current of 331.2 mA in the 7.5 M samples. In the 0.58 s/b ratio series, the 5.0 M samples experienced the highest current of 481.8 mA.

Similar to the amount of charge passed through these samples, the initial current flowing through these samples increased with increasing s/b ratios. The 10.0 M samples also showed the largest increases in current due to an increase in s/b ratio. When the s/b ratio was increased from 0.50 to 0.54, the current increased by 46.6%. When the s/b ratio was increased again from 0.54 to 0.58, the increase in current was 70.9%.

A consistent trend was recognized showing that with increasing s/b ratio, the amount of charge passed also increased. This trend matched what was experienced in Bondar et al.'s study. The alkali-activated natural pozzolan mixture made with a s/b ratio of 0.55 passed more charge than the mixture made with a 0.45 s/b ratio [17]. This indicates that s/b ratio affects the chloride ion penetration. Lower s/b ratios result in tighter pore structure, which is one of the most significant parameters involved in chloride penetration [17].

The NaOH concentration also affected the chloride penetration, however it did not follow a typical trend. The largest amount of charge was passed by the 7.5 M 0.58 s/b ratio samples, while the lowest charge passed was by the 12.5 M 0.54 s/b ratio samples. This trend is not related to those shown for compressive strength or absorption. It appears that the 5.0 M and 7.5

M samples pass the greatest amount of charge. At the lowest s/b ratio, the 5.0 M samples passed the greatest amount of charge, but as the s/b ratio increased, the 7.5 M samples surpassed the 5.0 M samples in terms of charge passed. This shows that as the s/b ratio increased, the mixture produced with more alkalis passed more charge. This trend did not continue to the 10.0 M and 12.5 M samples, most likely due to the level of bond formation experienced at those concentrations. Those samples achieved the largest compressive strengths, signifying the high level of activation. Furthermore, these samples had the smallest amount of voids, which may also prevent charge from passing through.

It should be noted that the RPCT measures the total electrical conductivity of the samples, which is dependent on the chemistry of the pore solution as well as the pore structure [17]. Any conducting ions present in the pore solution can increase the amount of charge passed through the sample [17]. This may have been responsible for the high charge passed through the 5.0 M and 7.5 M samples. These samples have greater alkali concentration than the 2.5 M samples, yet they do not provide as much activation as the 10.0 M and 12.5 M samples. This may lead to greater alkali presence within the pore solution, thus increasing the overall charge passed.

Bondar et al. also noted that the initial current can be used as a measure of the electrical conductivity of a sample [17]. The initial currents recorded show the largest values for the 5.0 M samples followed by the 7.5 M samples. This is related to the results shown for the amount of charge passed through the samples, indicating that these two mixtures have the highest electrical conductivity after 7 days of sealed curing.

4.6 Rapid Migration Test

The RMT test examined the physical chloride penetration depth of each sample. The migration coefficient, referred to as the DNSSM, is related to the rate of chloride penetration and chloride penetration depth. All three of the measurements exhibit the same trend so the focus of these results will be on the DNSSM. The results are summarized in Table 8 below.

Table 8: Average RMT Results

NaOH Concentration	S/B Ratio	DNSSM, x10 ⁻¹² (m ² /s)	Rate of Chloride Penetration (mm/Vh)	Chloride Penetration Depth (mm)
2.5 M	0.50	194.77	0.538	32.29
	0.54	214.57	0.587	35.19
	0.58	285.21	0.760	45.62
5.0 M	0.50	112.56	0.331	19.88
	0.54	121.01	0.352	21.09
	0.58	181.20	0.503	30.17
7.5 M	0.50	41.33	0.144	8.63
	0.54	64.55	0.206	12.38
	0.58	71.65	0.225	13.48
10.0 M	0.50	21.38	0.088	5.75
	0.54	21.80	0.089	5.33
	0.58	23.10	0.092	5.53
12.5 M	0.54	15.63	0.071	4.23
	0.58	17.08	0.075	4.49

Overall, the 2.5 M samples obtained the largest migration coefficients while the 12.5 M samples obtained the lowest migration coefficients. The 2.5 M 0.58 s/b ratio samples had a migration coefficient of 285.21 x 10⁻¹² m²/s which relates to a chloride penetration depth of 45.62 mm. The 12.5 M 0.54 s/b ratio samples had the greatest resistance to chloride, only attaining a migration coefficient of 15.63 x 10⁻¹² m²/s and a chloride penetration depth of 4.23 mm.

As the concentration was increased for each of the s/b ratios, the migration coefficient decreased. The greatest changes due to concentration for the 0.54 and 0.58 s/b ratio series occurred when the NaOH concentration was reduced from 10.0 M to 7.5 M. This increased the migration coefficients by 196% and 210% respectively. For the 0.50 s/b ratio series, the reduction in concentration from 7.5 M to 5.0 M led to the largest increase in migration coefficient, increasing the value by 172%. The effect of NaOH concentration on migration coefficient is seen in Figure 43.

The 10.0 M and 12.5 M samples showed little variation in migration coefficients due to increases in s/b ratios. The percent increases remained below 10% between consecutive s/b ratios. In contrast, the 2.5 M, 5.0 M, and 7.5 M samples showed much more significant increases in migration coefficients due to s/b ratio. The effect of s/b ratio on the migration coefficient is shown in Figure 44. The largest percent increase between samples was 56.2% due to the increase of s/b ratio from 0.50 to 0.54 for the 7.5 M samples.

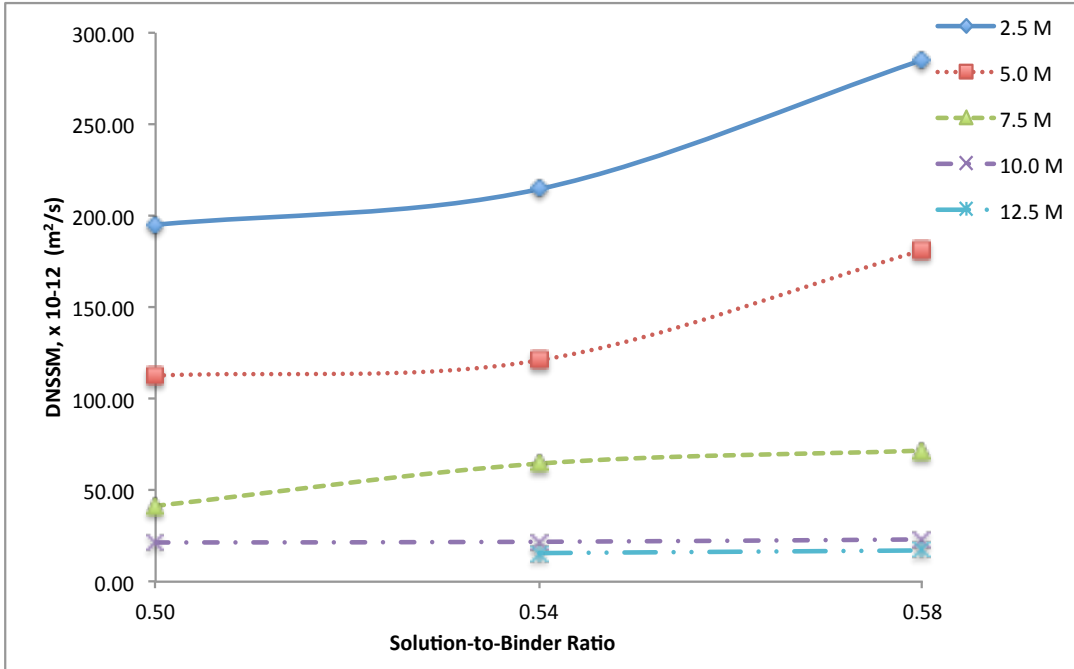


Figure 43: Effect of NaOH Concentration on 7-Day RMT Migration Coefficient

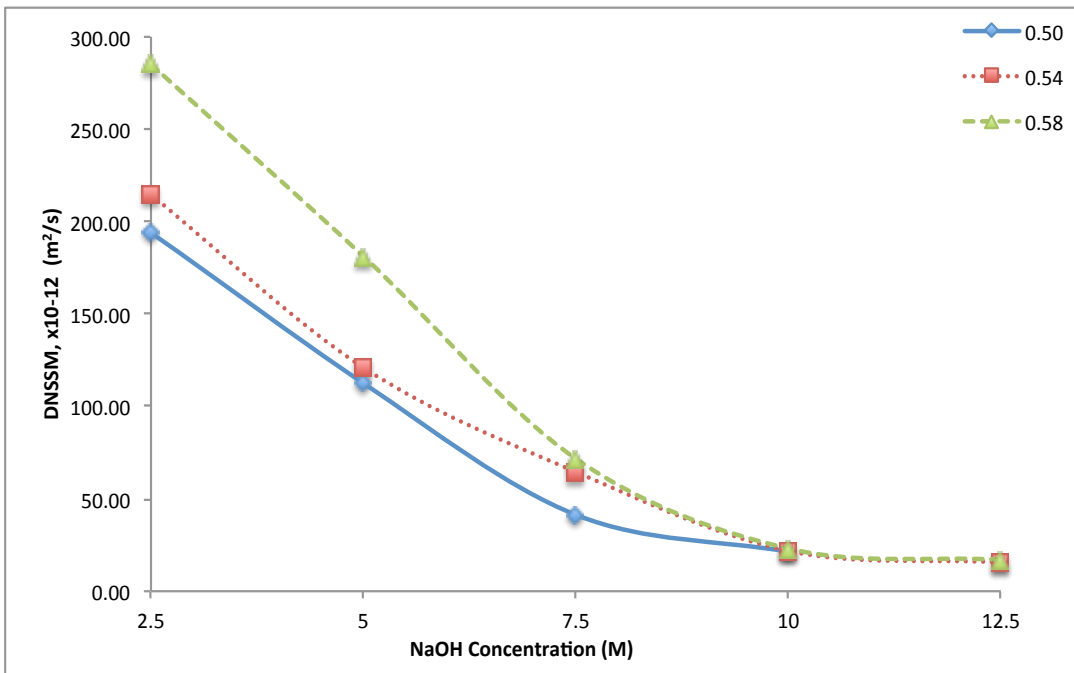


Figure 44: Effect of Solution-to-Binder Ratio on 7-Day RMT Migration Coefficient

The RMT is another method used to measure chloride penetration within a sample. The difference between this test and the RCPT is that the RMT provides results based on visual examination of the chloride penetration within the sample. The results achieved for the 7-day sealed curing samples showed different trends than the RCPT test results. The RMT results correspond well with the results seen for the compressive strengths of the samples. Increasing the NaOH concentration reduced the overall chloride penetration, as high concentrations allow for greater strength development. Additionally, reducing the s/b ratio also decreased the chloride penetration as lower s/b ratios create a tighter pore structure within the samples, reducing permeability [17]. This trend regarding the s/b ratios matches the trend seen in the RCPT results.

5. Conclusion and Recommendations

The mechanical strength performance and transport properties of alkali-activated natural pozzolans were evaluated for fourteen different mixtures. This study investigated the effects of curing environment, NaOH concentration, and s/b ratio on the flow; compressive and flexural strengths; density, absorption, and void content; and chloride penetration of natural pozzolans. Overall, natural pozzolans do have potential to act as OPC replacement materials in mortar and concrete. Based on this study, the most desirable mixture in terms of strength was the 12.5 M 0.58 s/b ratio mixture. After seven days of curing in the sealed condition, this mixture was able to exceed the structural compressive strength requirement of 20.7 MPa (3000 psi). The only drawback to this mixture is that it did not also achieve the lowest values for void content and chloride penetration. The 12.5 M mixture made with the lower s/b ratio of 0.54 had the lowest values for these conditions. However, the 12.5 M 0.58 s/b ratio mixture had much greater workability than the 0.54 s/b ratio mixture, making the former mixture easier to mix.

5.1 Fresh Properties – Flow and Density

The fresh densities for all mortar samples ranged from 2190 – 2525 kg/m³. The flow of mortar had an inverse relationship with NaOH concentration, while it had a direct relationship with s/b ratio.

5.2 Compressive Strength

The exposed curing environment allowed for the quickest strength gain due to the lack of humidity. After three days of curing, the exposed curing samples achieved their maximum compressive strengths. The sealed and moisture curing environments required longer curing times for samples to gain strength due to the presence of humidity. The moisture curing samples attained 59% to 76% of their ultimate compressive strengths after three days of curing while the sealed curing samples, with NaOH concentrations from 5.0 M to 12.5 M, attained 62% to 85% of their ultimate strengths. Overall, the sealed curing samples achieved the highest compressive strengths after seven days.

Increases in NaOH concentration produced samples with greater compressive strengths. These higher concentrations allowed for more aluminosilicate dissolution, resulting in improved performance.

S/b ratio had an inverse relationship on compressive strength. As the s/b ratio was increased, the compressive strength decreased, with the exception of the 12.5 M series of samples. The 12.5 M series performed better with the 0.58 s/b ratio because of the increased workability provided by the larger ratio.

Samples placed in the curing room for 7 and 28 days showed no significant strength gain. These samples would have little practical application within the construction industry due to the low compressive strengths achieved.

5.3 Flexural Strength

The flexural strength properties showed similar results to the compressive strength samples due to NaOH concentration and s/b ratio. Higher NaOH concentrations and lower s/b ratios produced samples with greater moduli of rupture and stiffness. The largest stiffness was exhibited by the 12.5 M sample with 0.54 s/b ratio and the smallest stiffness was shown by the 2.5 M 0.58 s/b ratio sample.

5.4 Density/Absorption/Voids

The densities of the 7-day sealed curing samples were shown to increase with increasing NaOH concentration. The absorption and void contents of the samples decreased with increasing NaOH concentration, while they were shown to increase with increasing s/b ratios.

5.5 Rapid Chloride Penetration Test

RCPT results showed that with increasing s/b ratio, more charge was passed through the 7-day sealed curing samples. The initial current was also shown to increase with increasing s/b ratio. The 7-day sealed curing samples showed the largest charge passing through the 5.0 M and 7.5 M samples.

5.6 Rapid Migration Test

The RMT results showed that the migration coefficient increased with increasing s/b ratios. Additionally, increasing the NaOH concentration reduced the migration coefficient.

5.7 Recommendations

When replacing OPC with alkali-activated natural pozzolans, the curing conditions drastically change. Instead of a moist environment, mortar made with natural pozzolans requires an elevated temperature and an environment that allows for some evaporation. The challenge with implementing a large-scale use of natural pozzolans within the construction industry is the limitations caused by this heated curing environment. Natural pozzolan usage may be limited to pre-cast mortar and concrete projects that are able to fit inside of an oven.

Another issue that needs to be addressed regarding natural pozzolan usage is the economic standpoint of using this material instead of OPC. Natural pozzolans are not available in every city around the world. They are mined from specific areas that had volcanic activity in the past. In contrast, OPC is able to be produced anywhere, making it much more readily available. If a city has natural pozzolan deposits, it may be a proactive idea to incorporate alkali-activated natural pozzolans in mortar and concrete mixes. However, if there is not a source nearby that produces natural pozzolans, the fee required to transport the pozzolans and the fossil fuels released along the way might counteract some of the benefits of using pozzolans.

Natural pozzolans also need a high curing temperature, requiring both money and energy. The OPC production process requires even higher temperatures, so there may be some savings on this end since these natural pozzolans are not heat treated in a kiln like OPC is. Another expense incurred by the usage of natural pozzolans is the cost of the alkali-activator, NaOH. If

used for a large project, several tons of NaOH may need to be purchased, thus increasing the overall cost of using natural pozzolans.

There are many ideas for future research on alkali-activated natural pozzolans. Firstly, research can be conducted to develop a super-plasticizer that will increase the workability of the mixtures. When using the higher NaOH concentrations, the mixture had reduced workability, making it difficult to mix. Currently, there are no available super-plasticizers that work in an alkali-activated environment. Secondly, research can be conducted on alkali-activated natural pozzolan concrete instead of mortar. The strength, load dependent properties, time dependent properties, and long-term durability of this type of concrete needs to be better understood. Finally, the last area of potential research involves the additions of various additives to help remove the need for oven curing.

There are many benefits to using alkali-activated natural pozzolans as replacements for OPC. There is potential for increased sustainability with no compromise to the material's mechanical and transport properties. However, the practicality of using natural pozzolans needs to be considered on a project-by-project basis. If the project site is near a source of natural pozzolans, incorporating them into the mortar or concrete may not increase overall costs. Additionally, if the project can be constructed from pre-cast bricks or similar small structures of mortar and concrete, natural pozzolans may suit the project well. Unfortunately, not all projects fall within those categories, thus limiting alkali-activated natural pozzolan usage.

6. Appendices

Appendix A: References

- [1] Huntzinger, Deborah N and Thomas D. Eatmon. “A life-cycle assessment of Portland cement manufacturing: comparing the traditional process with alternative technologies.” *Journal of Cleaner Production*, 17, 2009. 668-675.
- [2] Roy, Della M. “Alkali-activated cement opportunities and challenges.” *Cement and Concrete Research*, 29, 1999. 249-254.
- [3] Pacheco-Torgal, F.; Abdollahnejad, Z.; Camões, A.F.; Jamshidi, M.; Ding, Y. “Durability of alkali-activated binders: A clear advantage over Portland cement or an unproven issue?” *Construction and Building Materials*, 30, May 2012. 400-405.
- [4] Pacheco-Torgal, Fernando; Castro-Gomes, Joao; Jalali, Said. “Alkali-activated binders: A review: Part 1. Historical background, terminology, reaction mechanisms and hydration products.” *Construction and Building Materials*, 22, 2008. 1305-1314.
- [5] Jackson, Marie; Deocampo, Daniel; Marra, Fabrizio; Scheetz, Barry. “Mid-Pleistocene Pozzolan Volcanic Ash in Ancient Roman Concretes.” *Geoarchaeology: An International Journal*, 25, 2010. 36-74.
- [6] ACI Committee 232. “Use of Raw or Processed Natural Pozzolans in Concrete.” *American Concrete Institute*, 2001.
- [7] Winter, Nicholas B. *Understanding Cement*. Woodbridge, UK: WHD Microanalysis Consultants Ltd, 2012. Print.
- [8] Davidovits, J. “Synthesis of new high temperature geo-polymers for reinforced plastics/composites. *SPE PACTEC 79 Society of Plastic Engineers*, Brookfield Center, 1979. 151-154.

- [9] Khale, Divya and Chaudhary, Rubina. "Mechanism of geopolymerization and factors influencing its development: a review." *J Mater Sci*, 42, 2007. 729-746.
- [10] Kosmatka, Steven H.; Kerkhoff, Beatrix; Panarese, William C. "Design and Control of Concrete Mixtures." 14. Skokie, Illinois: Portland Cement Association, 2002.
- [11] Glukhovskiy, V.D.; Rostovskaja, G.S.; Rumyna, G.V. "High strength slag alkaline cements." *Proceedings of the seventh international congress on the chemistry of cement*, 3, 1980. 164-168.
- [12] Purdon, A.O. "The action of alkalis on blast furnace slag." *J Soc Chem Ind*, 59, 1940. 191-202.
- [13] Kani, Ebrahim Najafi and Ali Allahverdi. "Effects of curing time and temperature on strength development of inorganic polymeric binder based on natural pozzolan." *J Mater Sci*, 44, 2009. 3088-3097.
- [14] Lemougna, Patrick N; MacKenzie, Kenneth J.D.; Melo, U.F. Chinje. "Synthesis and thermal properties of inorganic polymers (geopolymers) for structural and refractory applications from volcanic ash." *Ceramics International*, 37, 8, 2011. 3011-3018.
- [15] Bondar, Dali; Lynsdale, C.J.; Milestone, Neil B.; Hassani, N.; Ramezani-pour, A.A. "Effect of type, form, and dosage of activators on strength of alkali-activated natural pozzolans." *Cement & Concrete Composites*, 33, 2011. 251-260.
- [16] Bondar, Dali; Lynsdale, Cyril J.; Milestone, Neil B.; Hassani, Nemat; Ramezani-pour, Ali Akbar. "Engineering Properties of Alkali-Activated Natural Pozzolan Concrete." *ACI Materials Journal*, 108, 2011. 64-72.

- [17] Bondar, Dali; Lynsdale, Cyril J.; Milestone, Neil B.; Hassani, Nemat. "Oxygen and Chloride Permeability of Alkali-Activated Natural Pozzolan Concrete." *ACI Materials Journal*, 109, 2012. 53-61.
- [18] Francis, Dana E. "Laboratory Test Report Class 'N' Pozzolan." Nevada Cement Company, June 2013.
- [19] Concrete-Materials Consultants, LLC. "Physical Properties of Fine Aggregate." Aggregate Industries, Inc., December 2011.
- [20] ASTM C1437-01. Standard Test Method for Flow of Hydraulic Cement Mortar. USA: American Society for Testing and Materials; 2001.
- [21] ASTM C109/C109M-02. Standard Test Method for Compressive Strength of Hydraulic Cement Mortars. USA: American Society for Testing and Materials; 2002.
- [22] ASTM C78-02. Standard Test Method for Flexural Strength of Concrete (Using Simple Beam with Third-Point Loading). USA: American Society for Testing and Materials; 2002.
- [23] ASTM C642-97. Standard Test Method for Density, Absorption, and Voids in Hardened Concrete. USA: American Society for Testing and Materials; 1997.
- [24] ASCM C1202-97. Standard Test Method for Electrical Indication of Concrete's Ability to Resist Chloride Ion Penetration. USA: American Society for Testing and Materials; 1997.
- [25] NT BUILD 492. Concrete, Mortar and Cement-Based Repair Materials: Chloride Migration Coefficient from Non-Steady-State Migration Experiments. NORDTEST; 1999.
- [26] Kosmatka, Steven H.; Kerkhoff, Beatrix; Panarese, William C. *Design and Control of Concrete Mixtures*. 14th. Skokie, Illinois: Portland Cement Association, 2002. Print.

Appendix B: Flow Data

Table 9: Flow Results

NaOH Concentration (M)	S/B Ratio	Flow (cm)
2.5	0.50	9.9
	0.54	13.0
	0.58	13.0
5.0	0.50	6.5
	0.54	8.3
	0.58	10.7
7.5	0.50	5.7
	0.54	7.5
	0.58	7.6
10.0	0.50	3.7
	0.54	5.0
	0.58	6.8
12.5	0.54	3.5
	0.58	5.7

Appendix C: Compressive Strength Data

Table 10: 2.5 M Compressive Strength Data

2.5 M Compressive Strengths				
S/B Ratio	Age (days)	Exposed (MPa)	Moisture (MPa)	Sealed (MPa)
0.50	1	3.775	4.159	4.718
	1	-	-	4.483
	1	-	-	4.552
	1	-	-	-
	3	4.912	6.202	5.433
	3	5.490	6.157	-
	3	-	-	-
	3	-	-	-
	7	4.614	9.974	6.052
	7	-	-	5.783
	7	-	-	5.774
	7	-	-	-
0.54	1	3.552	3.828	4.433
	1	3.558	4.411	4.566
	1	3.525	4.438	-
	1	-	-	-
	3	5.026	5.886	5.759
	3	5.057	-	5.624
	3	4.914	-	-
	3	4.926	-	-
	7	4.564	9.511	5.946
	7	4.581	9.514	5.552
	7	-	-	-
	7	-	-	-
0.58	1	2.204	2.775	2.615
	1	2.568	2.673	2.953
	1	-	2.499	3.080
	1	-	-	2.797
	3	3.123	4.349	3.394
	3	3.323	3.409	-
	3	2.299	-	-
	3	3.099	-	-
	7	2.620	6.284	4.161
	7	2.949	6.086	4.088
	7	3.146	5.853	3.401
	7	3.127	-	-

Table 11: 5.0 M Compressive Strength Data

5.0 M Compressive Strengths				
S/B Ratio	Age (days)	Exposed (MPa)	Moisture (MPa)	Sealed (MPa)
0.50	1	7.072	5.029	5.528
	1	7.360	4.985	4.828
	1	7.070	4.638	5.977
	1	7.272	4.500	5.250
	3	8.844	6.872	9.680
	3	9.145	7.966	-
	3	-	7.558	-
	3	-	-	-
	7	9.401	11.714	13.046
	7	8.292	10.707	12.362
	7	8.840	-	11.981
	7	8.835	-	-
0.54	1	6.088	4.126	4.364
	1	6.117	3.521	4.574
	1	5.924	4.125	4.145
	1	-	4.671	-
	3	6.653	6.851	8.201
	3	6.620	6.801	7.918
	3	-	-	9.104
	3	-	-	8.489
	7	6.948	10.655	11.496
	7	6.748	10.297	11.524
	7	6.710	-	11.095
	7	-	-	11.374
0.58	1	4.811	2.277	3.078
	1	4.487	2.136	2.994
	1	5.042	2.803	3.111
	1	4.612	2.585	2.890
	3	5.840	4.607	6.589
	3	5.817	4.428	7.039
	3	5.476	4.652	6.624
	3	4.931	-	-
	7	5.110	6.956	8.389
	7	5.124	-	8.596
	7	5.035	-	8.318
	7	5.076	-	-

Table 12: 7.5 M Compressive Strength Data

7.5 M Compressive Strengths				
S/B Ratio	Age (days)	Exposed (MPa)	Moisture (MPa)	Sealed (MPa)
0.50	1	12.096	6.667	7.360
	1	8.804	6.610	7.513
	1	9.854	-	7.287
	1	11.009	-	-
	3	15.147	10.381	16.779
	3	14.606	11.016	16.921
	3	13.734	12.096	15.886
	3	-	11.176	-
	7	16.593	17.339	21.319
	7	15.266	-	20.249
	7	13.954	-	20.075
	7	-	-	-
0.54	1	9.995	4.967	6.193
	1	9.447	5.057	5.557
	1	9.974	5.705	5.548
	1	-	5.550	6.065
	3	10.986	9.390	14.606
	3	-	9.564	14.895
	3	-	9.609	-
	3	-	8.375	-
	7	11.839	13.675	17.410
	7	11.212	-	19.480
	7	-	-	16.374
	7	-	-	18.367
0.58	1	8.168	3.178	3.504
	1	7.977	3.221	3.347
	1	8.194	3.404	3.589
	1	-	3.204	3.392
	3	10.073	6.917	15.900
	3	-	6.579	11.886
	3	-	5.964	10.385
	3	-	-	12.153
	7	8.577	8.549	14.668
	7	-	-	15.340
	7	-	-	14.620
	7	-	-	-

Table 13: 10.0 M Compressive Strength Data

10.0 M Compressive Strengths				
S/B Ratio	Age (days)	Exposed (MPa)	Moisture (MPa)	Sealed (MPa)
0.50	1	13.404	8.451	9.480
	1	13.696	7.913	9.409
	1	-	8.906	-
	1	-	9.473	-
	3	29.258	15.464	22.267
	3	28.210	15.704	-
	3	25.592	15.795	-
	3	-	16.741	-
	7	27.069	23.079	31.378
	7	27.355	21.524	32.447
	7	24.763	21.885	-
	7	25.489	24.977	-
0.54	1	13.689	6.267	7.889
	1	11.905	6.863	7.899
	1	-	6.931	-
	1	-	6.762	-
	3	24.841	15.116	21.581
	3	20.921	15.161	-
	3	27.740	12.565	-
	3	27.667	11.097	-
	7	24.070	21.564	26.204
	7	26.769	22.136	30.229
	7	21.948	20.166	-
	7	23.974	20.621	-
0.58	1	15.275	5.145	6.036
	1	11.803	4.778	5.602
	1	9.228	5.047	5.540
	1	11.253	5.004	5.612
	3	25.473	8.859	17.226
	3	20.621	8.735	17.841
	3	22.260	9.095	-
	3	19.406	-	-
	7	21.848	14.797	27.095
	7	23.151	15.209	-
	7	19.737	-	-
	7	-	-	-

Table 14: 12.5 M Compressive Strength Data

12.5 M Compressive Strengths				
S/B Ratio	Age (days)	Exposed (MPa)	Moisture (MPa)	Sealed (MPa)
0.54	1	14.689	7.642	11.166
	1	17.324	6.617	11.600
	1	14.954	7.330	9.600
	1	15.805	7.511	9.087
	3	31.594	15.799	23.901
	3	30.639	15.666	24.270
	3	31.439	17.391	-
	3	29.522	16.229	-
	7	27.660	24.932	30.827
	7	27.517	26.380	-
	7	-	-	-
	7	-	-	-
0.58	1	14.682	5.653	7.274
	1	13.398	5.583	6.901
	1	-	5.498	7.829
	1	-	6.076	7.546
	3	30.191	16.278	22.722
	3	31.504	17.152	22.143
	3	36.925	18.692	20.533
	3	30.923	17.293	27.841
	7	31.278	26.621	37.202
	7	33.367	-	38.190
	7	32.793	-	-
	7	29.684	-	-

Appendix D: Density/Absorption/Void Data

Table 15: 0.50 S/B Ratio Density/Absorption/Void Data

Concentration	S/B Ratio	Sample #	Abs. after immers. (%)	Abs. after immers and boiling (%)	Bulk density, dry	Bulk density after immers.	Bulk density after immers. and boiling	App. Density	Volume of Perm. Pore space, voids
2.5 M	0.50	1	12.28%	13.41%	1.914	2.149	2.171	2.575	25.67%
		2	12.49%	13.78%	1.874	2.108	2.132	2.525	25.81%
		3	12.43%	13.67%	1.905	2.142	2.165	2.575	26.04%
		Average	12.40%	13.62%	1.898	2.133	2.156	2.559	25.84%
5 M	0.50	1	10.39%	11.95%	1.939	2.140	2.170	2.523	23.17%
		2	10.65%	12.28%	1.934	2.140	2.171	2.536	23.74%
		3	9.94%	11.22%	1.956	2.151	2.176	2.506	21.95%
		Average	10.33%	11.82%	1.943	2.144	2.172	2.522	22.95%
7.5 M	0.50	1	7.61%	8.29%	2.076	2.234	2.248	2.507	17.21%
		2	7.41%	8.04%	2.087	2.242	2.255	2.508	16.79%
		3	8.08%	8.94%	2.059	2.226	2.243	2.524	18.41%
		Average	7.70%	8.42%	2.074	2.234	2.249	2.513	17.47%
10 M	0.50	1	8.23%	9.56%	2.018	2.184	2.211	2.500	19.29%
		2	-0.12%	0.39%	2.178	2.175	2.186	2.196	0.84%
		3	3.71%	4.04%	2.103	2.181	2.188	2.298	8.50%
		Average	3.94%	4.66%	2.100	2.180	2.195	2.332	9.54%

Table 16: 0.54 S/B Ratio Density/Absorption/Void Data

Concentration	S/B Ratio	Sample #	Abs. after immers. (%)	Abs. after immers and boiling (%)	Bulk density, dry	Bulk density after immers.	Bulk density after immers. and boiling	App. Density	Volume of Perm. Pore space, voids
2.5 M	0.54	1	13.35%	15.19%	1.881	2.132	2.167	2.634	28.58%
		2	13.49%	15.27%	1.879	2.132	2.166	2.634	28.69%
		3	13.38%	15.38%	1.871	2.122	2.159	2.628	28.78%
		Average	13.41%	15.28%	1.877	2.129	2.164	2.632	28.68%
5 M	0.54	1	11.46%	13.07%	1.903	2.122	2.152	2.534	24.88%
		2	11.05%	12.70%	1.860	2.065	2.096	2.435	23.62%
		Average	11.26%	12.88%	1.903	2.094	2.124	2.484	24.25%
7.5 M	0.54	1	8.61%	9.44%	1.962	2.130	2.147	2.407	18.52%
		2	8.58%	9.39%	1.938	2.105	2.120	2.370	18.21%
		3	8.05%	9.30%	1.928	2.083	2.107	2.349	17.93%
		Average	8.42%	9.38%	1.962	2.106	2.125	2.389	18.22%
10 M	0.54	1	4.82%	6.97%	2.028	2.125	2.169	2.362	14.13%
		2	6.50%	8.04%	2.040	2.173	2.204	2.440	16.40%
		3	5.08%	6.99%	2.045	2.149	2.188	2.386	14.30%
		Average	5.47%	7.33%	2.038	2.149	2.187	2.374	14.94%
12.5 M	0.54	1	2.00%	3.96%	2.066	2.108	2.148	2.250	8.17%
		2	3.13%	6.08%	2.060	2.124	2.185	2.354	12.52%
		3	2.00%	3.04%	2.088	2.129	2.151	2.229	6.35%
		Average	2.38%	4.36%	2.071	2.120	2.161	2.278	9.01%

Table 17: 0.58 S/B Ratio Density/Absorption/Void Data

Concentration	S/B Ratio	Sample #	Abs. after immers. (%)	Abs. after immers and boiling (%)	Bulk density, dry	Bulk density after immers.	Bulk density after immers. and boiling	App. Density	Volume of Perm. Pore space, voids
2.5 M	0.58	1	13.99%	15.89%	1.842	2.099	2.134	2.604	29.26%
		2	13.95%	15.79%	1.833	2.088	2.122	2.579	28.94%
		3	13.53%	15.32%	1.847	2.096	2.129	2.575	28.28%
		Average	13.82%	15.66%	1.840	2.095	2.129	2.586	28.83%
5 M	0.58	1	11.40%	13.16%	1.906	2.123	2.157	2.544	25.09%
		2	11.58%	13.15%	1.916	2.138	2.168	2.561	25.19%
		3	11.57%	13.21%	1.907	2.128	2.159	2.550	25.19%
		Average	11.52%	13.17%	1.907	2.130	2.161	2.552	25.16%
7.5 M	0.58	1	10.14%	12.37%	1.981	2.182	2.226	2.624	24.51%
		2	9.54%	11.78%	1.961	2.148	2.192	2.550	23.10%
		3	10.07%	12.37%	1.975	2.174	2.219	2.614	24.43%
		Average	9.92%	12.17%	1.961	2.168	2.213	2.550	24.01%
10 M	0.58	1	5.84%	9.75%	1.952	2.066	2.143	2.411	19.03%
		2	6.26%	8.62%	1.947	2.069	2.114	2.339	16.77%
		3	7.13%	9.07%	1.984	2.125	2.164	2.419	17.99%
		Average	6.41%	9.14%	1.961	2.087	2.140	2.390	17.93%
12.5 M	0.58	1	2.62%	5.71%	2.070	2.124	2.188	2.347	11.81%
		2	2.46%	6.21%	2.042	2.092	2.169	2.339	12.69%
		3	2.15%	5.18%	2.095	2.140	2.204	2.350	10.86%
		Average	2.41%	5.70%	2.069	2.119	2.187	2.345	11.78%

Appendix E: RCPT Data

Table 18: RCPT Data

NaOH Concentration	Initial Current (mA)			Adjusted Charge Passed (Coulombs)		
	0.50	0.54	0.58	0.50	0.54	0.58
2.5	263.8	315.9	369.3	6069	6162	7799
	276.8	276.5	344.3	6166	5780	5801
	-	304.9	-	-	6983	-
5.0	374.6	---	481.8	6625	---	6776
	-	---	-	-	---	-
	-	---	-	-	---	-
7.5	334.5	331.2	439.0	6239	6433	7080
	-	-	-	-	-	-
	-	-	-	-	-	-
10.0	115.2	195.2	328.3	2202	3459	6788
	133.6	169.5	295.1	2611	3467	6005
	-	-	-	-	-	-
12.5	N/A	43.9	57.5	N/A	868	867
	N/A	58.3	67.0	N/A	1078	1260
	N/A	64.2	-	N/A	1217	-

Appendix F: RMT Data

Table 19: 2.5 M RMT Chloride Penetration Depth Data

2.5 M Chloride Penetration Depths at Given Distances (mm)							
S/B Ratio	20 mm	30 mm	40 mm	50 mm	60 mm	70 mm	80 mm
0.50	28.84	30.68	30.95	32.65	34.43	31.87	32.18
	32.25	31.96	30.31	32.18	32.86	32.31	32.60
	34.51	34.07	31.59	32.65	32.89	32.83	33.41
0.54	36.7	39.57	33.4	33.13	32.84	36.09	34.6
	-	-	-	-	-	-	-
	-	-	-	-	-	-	-
0.58	45.74	46.02	48.38	47.12	47.23	47.02	47.91
	45.48	46.23	46.78	47.28	47.02	46.48	46.90
	45.92	43.67	42.68	43.13	42.91	41.96	42.08

Table 20: 5.0 M RMT Chloride Penetration Depth Data

5.0 M Chloride Penetration Depths at Given Distances (mm)							
S/B Ratio	20 mm	30 mm	40 mm	50 mm	60 mm	70 mm	80 mm
0.50	16.55	17.08	18.18	18.57	18.31	18.48	20.19
	20.14	20.91	18.46	18.98	18.91	18.61	20.60
	22.10	21.62	21.64	21.53	22.15	22.54	21.92
0.54	19.3802	22.58	19.74	23.09	25.17	30.07	28.80
	19.18	22.12	17.88	13.82	16.84	23.60	21.16
	18.08	19.58	18.08	20.27	18.49	20.07	24.94
0.58	28.09	26.97	31.98	33.46	28.98	29.25	25.07
	31.17	29.15	29.86	27.47	27.40	27.86	33.69
	29.28	31.20	34.75	33.90	32.32	30.29	31.53

Table 21: 7.5 M RMT Chloride Penetration Depth Data

7.5 M Chloride Penetration Depths at Given Distances (mm)							
S/B Ratio	20 mm	30 mm	40 mm	50 mm	60 mm	70 mm	80 mm
0.50	10.40	8.61	8.31	8.66	8.47	8.70	8.28
	8.70	7.92	8.26	8.67	8.55	8.69	8.79
	8.65	8.53	8.54	8.96	8.55	8.42	8.56
0.54	12.50	12.83	12.32	11.91	12.47	11.48	11.05
	20.88	13.06	13.54	11.89	11.58	14.81	14.05
	13.00	16.54	10.21	7.39	8.56	7.80	12.09
0.58	11.25	10.43	9.61	10.29	10.64	12.35	14.83
	12.83	13.24	12.85	12.95	14.01	15.49	19.28
	15.38	16.81	15.46	14.84	12.41	13.32	14.90

Table 22: 10.0 M RMT Chloride Penetration Depth Data

10.0 M Chloride Penetration Depths at Given Distances (mm)							
S/B Ratio	20 mm	30 mm	40 mm	50 mm	60 mm	70 mm	80 mm
0.50	6.62	6.30	6.78	6.22	6.46	6.31	8.33
	5.41	5.55	5.46	5.22	5.24	5.54	5.44
	5.46	4.76	5.10	5.26	4.87	5.15	5.18
0.54	3.78	5.25	5.71	6.86	5.72	5.43	5.79
	6.80	4.15	5.33	3.72	4.47	5.08	6.53
	-	-	-	-	-	-	-
0.58	5.66	4.32	4.18	3.65	4.75	4.27	5.34
	4.57	4.20	4.14	3.86	4.01	5.29	5.86
	8.32	8.35	6.97	4.31	5.54	7.92	10.58

Table 23: 12.5 M RMT Chloride Penetration Depth Data

12.5 M Chloride Penetration Depths at Given Distances (mm)							
S/B Ratio	20 mm	30 mm	40 mm	50 mm	60 mm	70 mm	80 mm
0.54	3.89	6.13	4.05	3.96	3.94	3.15	4.47
	4.07	4.49	3.29	3.39	4.61	4.95	4.87
	-	-	-	-	-	-	-
0.58	5.41	4.02	4.26	3.73	4.25	4.60	5.66
	5.09	3.76	4.02	4.90	5.16	5.06	4.27
	4.37	4.26	4.30	3.91	4.57	4.28	4.39

Table 24: 2.5 M Rates of Chloride Penetration Data

2.5 M Rates of Chloride Penetration		
S/B Ratio	DNSSM, x10 ⁻¹² (m ² /s)	Rate of Chloride Penetration (mm/Vh)
0.50	190.56	0.528
	193.30	0.534
	200.46	0.552
0.54	214.57	0.587
	-	-
	-	-
0.58	295.04	0.784
	291.88	0.777
	268.72	0.720

Table 25: 5.0 M Rates of Chloride Penetration Data

5.0 M Rates of Chloride Penetration		
S/B Ratio	DNSSM, x10 ⁻¹² (m ² /s)	Rate of Chloride Penetration (mm/Vh)
0.50	101.61	0.303
	110.17	0.325
	125.90	0.365
0.54	140.90	0.402
	108.77	0.320
	113.36	0.332
0.58	174.10	0.485
	176.78	0.492
	192.73	0.532

Table 26: 7.5 M Rates of Chloride Penetration Data

7.5 M Rates of Chloride Penetration		
S/B Ratio	DNSSM, x10 ⁻¹² (m ² /s)	Rate of Chloride Penetration (mm/Vh)
0.50	42.22	0.146
	40.61	0.142
	41.16	0.143
0.54	62.63	0.201
	76.37	0.238
	54.64	0.180
0.58	58.10	0.189
	77.35	0.240
	79.49	0.246

Table 27: 10.0 M Rates of Chloride Penetration Data

10.0 M Rates of Chloride Penetration		
S/B Ratio	DNSSM, x10 ⁻¹² (m ² /s)	Rate of Chloride Penetration (mm/Vh)
0.50	22.22	0.090
	20.53	0.085
	-	-
0.54	22.80	0.092
	20.79	0.086
	-	-
0.58	17.68	0.077
	17.49	0.076
	34.13	0.124

Table 28: 12.5 M Rates of Chloride Penetration Data

12.5 M Rates of Chloride Penetration		
S/B Ratio	DNSSM, x10⁻¹² (m²/s)	Rate of Chloride Penetration (mm/Vh)
0.54	15.60	0.070
	15.66	0.071
	-	-
0.58	17.49	0.076
	17.75	0.077
	16.01	0.072